Novel Benzazole Derivatives Endowed with Potent Antiheparanase Activity

Journal of Medicinal Chemistry

Article

Novel Benzazole Derivatives Endowed with Potent anti-Heparanase Activity

Valentina Noemi Madia, Antonella Messore, Luca Pescatori, Francesco Saccoliti, Valeria Tudino, Alessandro De Leo, Martina Bortolami, Luigi Scipione, Roberta Costi, Silvia Rivara, Laura Scalvini, Marco Mor, Fabiana Fosca Ferrara, Emiliano Pavoni, Giuseppe Roscilli, Giuliana Cassinelli, Ferdinando M Milazzo, Gianfranco Battistuzzi, Roberto Di Santo, and Giuseppe Giannini

J. Med. Chem., **Just Accepted Manuscript** • DOI: 10.1021/acs.jmedchem.8b00908 • Publication Date (Web): 16 Jul 2018

ACS Publications

is published by the American Chemical Society. 1155 Sixteenth Street N.W., Washington, DC 20036

Novel Benzazole Derivatives Endowed with Potent anti-Heparanase Activity

Valentina Noemi Madia,[a] Antonella Messore,[a] Luca Pescatori,[a] Francesco Saccoliti,[a] Valeria Tudino,[a] Alessandro De Leo,[a] Martina Bortolami,[a] Luigi Scipione,[a] Roberta Costi,[a] Silvia Rivara,[b] Laura Scalvini,[b] Marco Mor,[b] Fabiana Fosca Ferrara,[c] Emiliano Pavoni,[c] Giuseppe Roscilli,[c] Giuliana Cassinelli,[d°] Ferdinando M. Milazzo,[e°] Gianfranco Battistuzzi,[e°] Roberto Di Santo[a] and Giuseppe Giannini[e°*]*

[a] Dipartimento di Chimica e Tecnologie del Farmaco, Istituto Pasteur-Fondazione Cenci Bolognetti, "Sapienza" Università di Roma, p.le Aldo Moro 5, I-00185, Roma Italy

[b] Dipartimento di Scienze degli Alimenti e del Farmaco, Università degli Studi di Parma, Parco Area delle Scienze 27/A, I- 43124 Parma, Italy

[c] Takis s.r.l., Via Castel Romano 100, I-00128 Roma, Italy

[d] Dipartimento di Ricerca Applicata e Sviluppo Tecnologico, Unità di Farmacologia Molecolare, Fondazione IRCCS Istituto Nazionale dei Tumori, via Amadeo 42, I-20133 Milano, Italy

[e] R&D Alfasigma S.p.A., Via Pontina Km 30,400, Pomezia, I-00071Roma, Italy

KEYWORDS. Heparanase, Heparanase inhibitors, Anticancer agents, Angiogenesis, Benzimidazole, Benzoxazole.

°Note: Activity carried out within a collaborative research agreement with Leadiant Biosciences S.A. (Formerly Sigma-Tau Research Switzerland, S.A.), Mendrisio, CH.

ABSTRACT

Heparanase is the sole mammalian enzyme capable of cleaving glycosaminoglycan heparan sulfate side chains of heparan sulfate proteoglycans. Its altered activity is intimately associated with tumor growth, angiogenesis and metastasis. Thus, its implication in cancer progression makes it an attractive target in anticancer therapy. Herein, we describe the design, synthesis and biological evaluation of new benzazoles as heparanase inhibitors. Most part of designed derivatives were active at micromolar or submicromolar concentration and the most promising compounds are fluorinated and/or amino acids derivatives **13a**, **14d** and **15** that showed IC_{50} 0.16-0.82 μM. Molecular docking studies were performed to rationalize their interaction with the enzyme catalytic site. Importantly, invasion assay confirmed the anti-metastatic potential of compounds **14d** and **15**. Consistent with its ability to inhibit heparanase, compound **15** proved to decrease expression of genes encoding for proangiogenic factors such as MMP-9, VEGF and FGFs in tumor cells.

Introduction

Heparanase (Hpse) is the only mammalian enzyme endowed with *endo*-β-D-glucuronidase activity. It cleaves glycosaminoglycan heparan sulfate (HS) side chains of heparan sulfate proteoglycans (HSPGs) at a limited number of sites, by catalyzing the hydrolysis of the β-glycosidic bond at specific intrachain sites with retention of the anomeric configuration.[1] HSPGs are a class of glycoproteins predominantly localized on cell surface, in the basement membrane (BM) and in the extracellular matrix (ECM) of a wide cellular range of both vertebrate and invertebrate tissues.[2] This class of nearly-ubiquitous macromolecules is mainly involved in key biological processes like cell adhesion, growth and motility/invasion as well as in ECM assembly and growth factor storage. Indeed, physiologically these actions are ~~all~~ regulated by the interactions of the HS-side chains with a variety of proteins including cytokines, lipoproteins, growth factors along with their receptors, and enzymes involved in inflammation and wound healing repair.[3-6] Hpse not only influences a multitude of physiological processes but it is involved in several cancer- and inflammatory-based diseases such as chronic inflammation, atherosclerosis, thrombosis, fibrosis, in the neuronal process known as neurite outgrowth, diabetic nephropathy and bone osteolysis.[7-9] Up-regulated expression and altered activity have been reported for Hpse in a variety of human hematological and solid malignancies, for example, pancreatic, ovarian, bladder, brain, colon, prostate, breast, liver cancers, myeloma and sarcoma.[10,11] Several clinical studies have demonstrated that Hpse up-regulation is associated with growth/aggressiveness of numerous cancer cell types and, clinically it is consistently correlated with an increase in tumor size, enhancement of tumor progression, metastasis and poor prognosis.[12] Thus, when Hpse is overexpressed, it turns into a tumor marker, contributing to tumor associated pathological conditions like tissue inflammation, angiogenesis and distant

dissemination. Importantly, there is only a single enzymatically active form of Hpse in humans, that is poorly expressed in normal tissues, and Hpse knockout animals exhibit no obvious deficits,[12] implying that its inhibition will cause minimal side effects in patients that could benefit of a putative anti-Hpse therapy. Preclinical studies showed that knockdown of Hpse expression or treatment of tumor-bearing mice with Hpse inhibitors significantly impair tumor progression, thus highlighting the potential of Hpse as a valuable druggable target for anticancer therapy.[13]

Besides, Hpse promotes autophagy and several lines of evidence implicate its expression in chemoresistance.[14] Overall, Hpse represents an attractive and promising target for innovative pharmacological applications. In view of the above, compounds able to specifically modulate the expression or activity of this enzyme are highly desired and explored as a useful pharmacological option for those clinical indications in which Hpse inhibition could be pharmacologically useful with particular reference to oncological diseases. However, although in the last twenty years numerous efforts have been made in this sense and huge progresses have been achieved in the knowledge of Hpse activity and functions, among the several classes of inhibitors that have been described so far, no drug able to inhibit or modulate Hpse functions has yet been registered.[1,15-18] The search for molecules able to interfere with Hpse biological activities has led to the discovery of several inhibitors, both synthetic and of natural origin, ranging from heparin-derivatives and polysulfated oligosaccharides, nucleic acids, proteins, monoclonal antibodies to small-molecule inhibitors. Among them, only four drugs have so far reached different phases of clinical trials as anti-cancer agents. They are polysaccharide derivatives of natural origin, such as roneparstat (**1**, SST0001), necuparanib (**2**, M-402) and muparfostat (**3**, PI-88), or obtained by synthesis as pixatimod (**4**, PG545)[1] Such polysulfated polysaccharides share various limitations, related not only to their high molecular weight and heterogeneous nature (both in chain length and

composition) that could limit product characterization, standardization and interpretation of biological data, but also to their parenteral delivery route that may affect the patient compliance. Small molecules are instead particularly desirable due to their more favorable pharmacokinetic properties. Furthermore, they can be optimized for oral administration thus resulting in an improved patient therapeutic compliance. Although various attempts have been made over time to select and develop a drug with suitable properties, to date no small molecule able to inhibit Hpse activity has ever entered clinical trials.

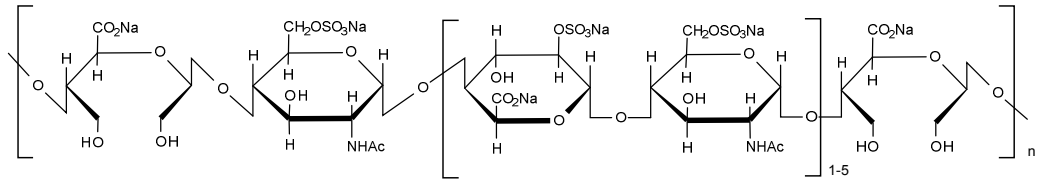

1

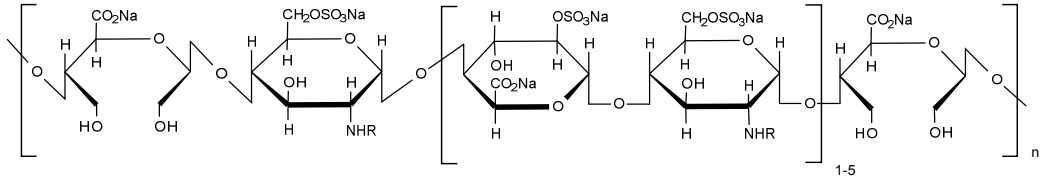

R = SO_3Na or Ac

2

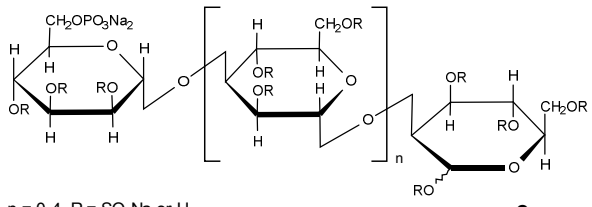

n = 0-4, R = SO_3Na or H

3

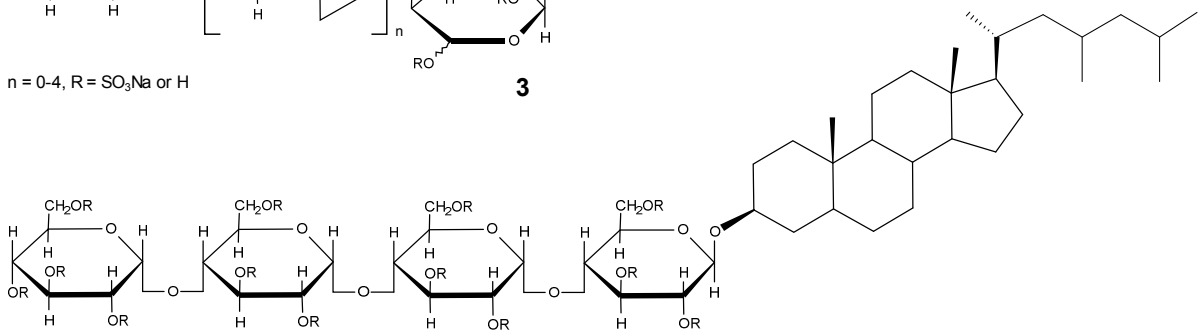

R = SO_3Na

4

Figure 1. Hpse inhibitors in clinical trials roneparstat (**1**, SST0001), necuparanib (**2**, M-402), muparfostat (**3**, PI-88), and pixatimod (**4**, PG545).

During the last decade, new series of Hpse inhibitors based on benzimidazol-2-yl scaffold were reported, with some derivatives (e.g. **5**, **6**, Figure 2) endowed with good inhibitory potencies (IC_{50} of 0.91 and 0.23 μM, respectively).[19,20] Furthermore, benzoxazol-5-yl acetic acid derivatives have been described for their anti-Hpse activity (**7**, **8** with IC_{50} of 0.75 and 3.0 μM, respectively).[21,22]

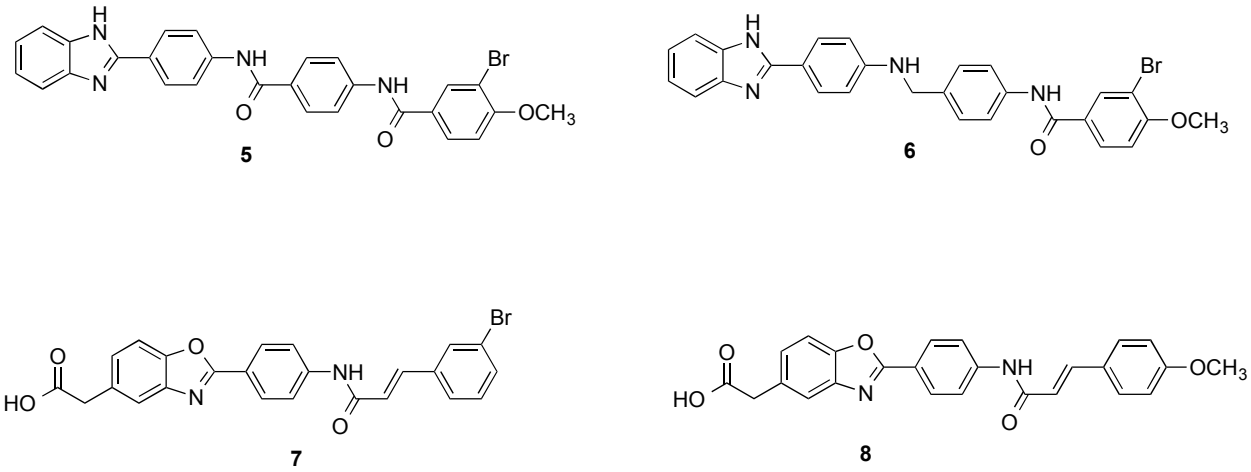

Figure 2. Chemical structures of benzazole Hpse inhibitors.

Taking into account all above mentioned as prior-art, we designed, synthesized and biologically evaluated new benzoxazole and benzimidazole derivatives structurally related to anti-Hpse agents **5-8** (Chart 1). First, we fused structures of compounds **6** and **7** designing benzimidazoles **9** and benzoxazoles **10**. These new compounds are characterized by both the scaffold of compound **6** and the acetic portion of inhibitor **7**. However, benzimidazoles **9** and benzoxazoles **10** are more extended molecules if compared to the corresponding counterpart **6**

and **7**, respectively, and were designed to better fit the long substrate binding pocket of Hpse. Again a similar approach was exploited for compounds **13** and **14**, the amino acid derivatives of **9** and **10**, in which the further increase of molecular length obtained by linking amino acid residues to the acetic chain, gave compounds with side chain endowed of increased degrees of freedom (Chart 1). As particular cases of amino acid branches, also the boronic derivatives **13d** and **14f** were studied, as groups that potentially replace the carboxylate portion of **13a** and **14a**, respectively.

Chart 1. Design of the New Benzazole Derivatives **9**, **10**, **13**, and **14**.

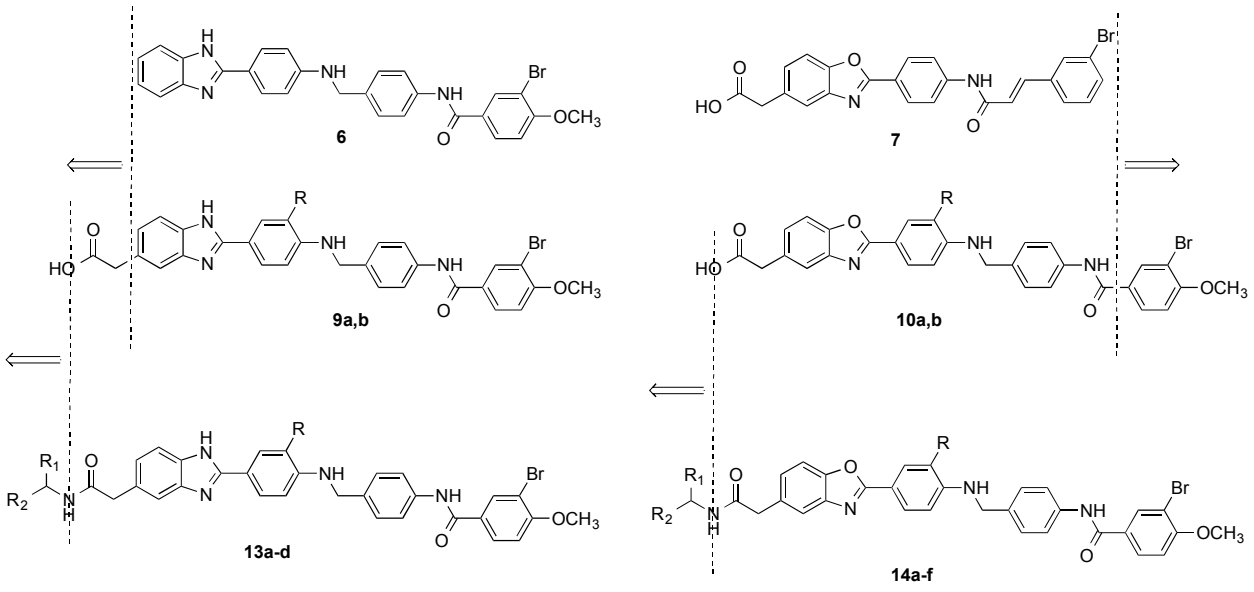

We designed the new derivatives **9**, **10**, **13** and **14** introducing a fluorine atom on the phenyl ring linked to the benzazole core in ortho position to the amino group, since this atom can give higher potency against Hpse as suggested by literature data.[21] In particular, we synthesized benzimidazole derivative **15** as fluoro derivative counterpart of compound **6.** The unfluorinated

compounds **9b** and **10b** were specifically designed as reference compounds to prove the important role of the fluorine atom in improving the anti Hpse activity. Finally, we synthesized the pseudo-symmetric derivative **10c** characterized by a second benzoxazole acetic group replacing the bromo-methoxybenzamide moiety of derivatives **9**, **10**, **13** and **14** (Chart 2). This substitution can allow to scan the possibility of further polar interactions of the second carboxylate with the hydrophilic pocket of the target.

Chart 2. Structures of the Newly Designed Benzazole Derivatives **9a,b, 10a-c, 13a-d, 14a-f, 15**

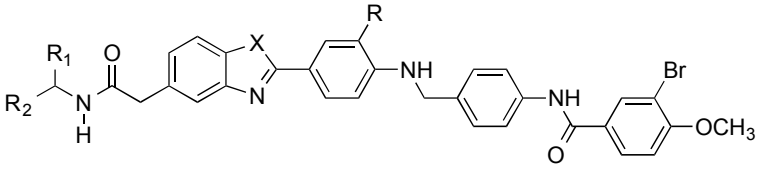

13a X=NH, R=F, R_1=H, R_2=COOH
13b X=NH, R=F, R_1=CH_3, R_2=COOH
13c X=NH, R=F, R_1=CH_2Ph, R_2=COOH
13d X=NH, R=F, R_1=H, R_2=$B(OH)_2$
14a X=O, R=F, R_1=H, R_2=COOH
14b X=O, R=F, R_1=CH_3, R_2=COOH
14c X=O, R=F, R_1=CH_2Ph, R_2=COOH
14d X=O, R=F, R_1=CH_2CH_2COOH, R_2=COOH
14e X=O, R=F, R_1=$(CH_2)_4NH_2$, R_2=COOH
14f X=O, R=F, R_1=H, R_2=$B(OH)_2$

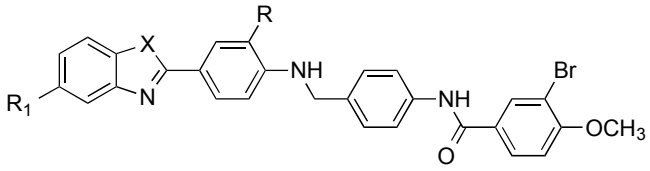

9a X=NH, R=F, R_1=CH_2COOH
9b X=NH, R=H, R_1=CH_2COOH
10a X=O, R=F, R_1=CH_2COOH
10b X=O, R=H, R_1=CH_2COOH
15 X=NH, R=F, R_1=H

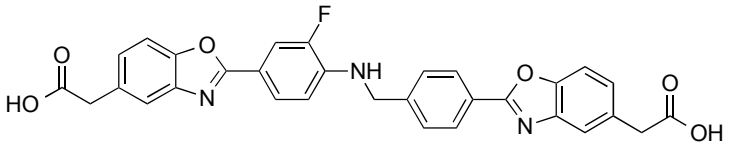

10c

The newly synthesized compounds have been evaluated in vitro for their ability to inhibit Hpse enzymatic activity and to affect behaviors associated with tumor cell malignant phenotype such as cell proliferation and invasive potential. In addition, the effect of a selected compound on expression of genes encoding for proangiogenic factors have been measured in tumor cells.

Moreover, a rationalization of the interaction with the biological target has been proposed, based on docking studies using the crystal structure of human Hpse.

Results and discussion

Chemistry. The benzazole derivatives, **9a,b, 10a,b, 13a-c** and **14a-e**, were synthesized as reported in Scheme 1. The intermediates **17a** and **17b** were obtained from methyl 2-(3,4-diaminophenyl)acetate **16**[23] that underwent to condensation with the proper commercially available 4-nitrobenzaldehyde in the presence of ceric ammonium nitrate (CAN) and H_2O_2 30%[24]. Imino derivatives **20a,b** and **21a,b** were obtained by condensation of the corresponding amines **18a,b** (obtained from the corresponding nitro derivatives **17a** and **17b** under Leuckart reduction conditions) and **19a,b**[22] with 3-bromo-*N*-(4-formylphenyl)-4-methoxybenzamide[20], which were reduced to the corresponding benzylamino derivatives **22a,b** and **23a,b** in the presence of sodium borohydride. Subsequent alkaline hydrolysis with LiOH gave the corresponding acid derivatives **9a,b** and **10a,b**. The latter compounds underwent coupling reactions with the proper amino ester in the presence of 1-ethyl-3-(3-dimethylaminopropyl)carbodiimide hydrochloride (EDCI) and 4-dimethylaminopyridine (DMAP) using *N*,*N*-diisopropylethylamine (DIPEA) as base to give esters **11a,b** and **12a,b** that were in turn hydrolyzed in alkaline medium to give the corresponding amino acid derivatives **13a-c** and **14a-d**. Derivative **14e** was preliminarily Fmoc-deprotected in the presence of piperidine 20% in DMF.[24]

Scheme 1. Synthetic Route to **9a,b, 10a,b, 13a-c** and **14a-e** Derivatives[a]

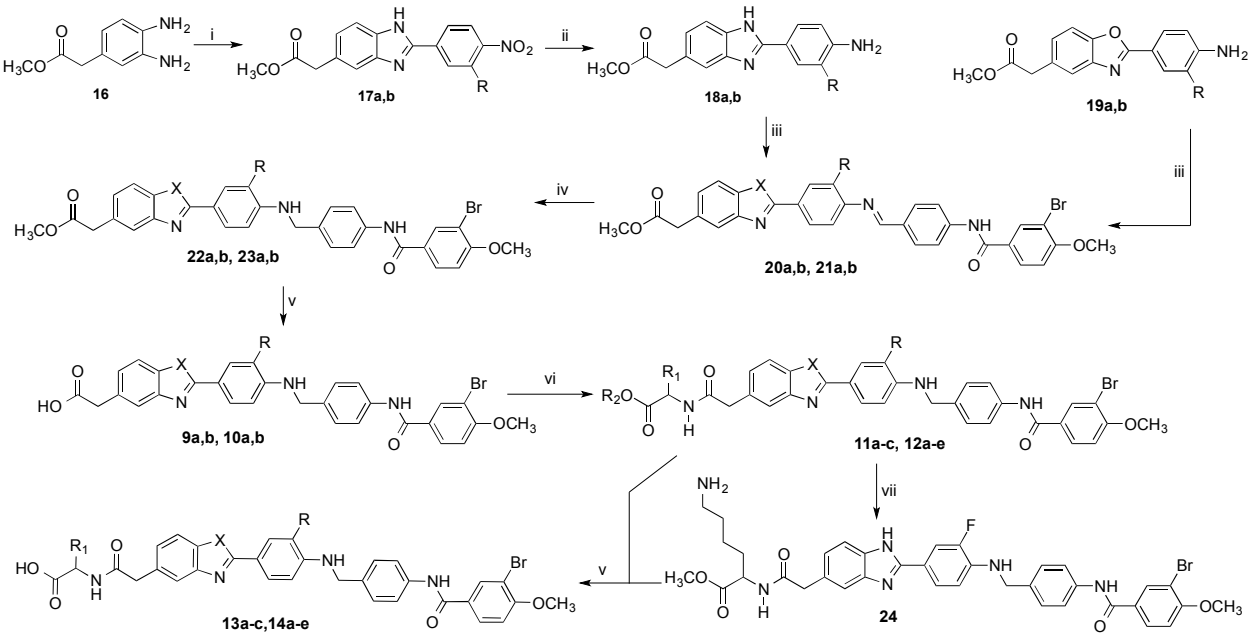

[a] Reagents and conditions: (i) proper aldehyde reagent, CAN, H_2O_2 30%, MeCN dry, N_2, 50 °C, 50 min, 65-69% yield; (ii) ammonium formate, $NHEt_2$, Pd/C, AcOEt or MeOH, N_2, reflux, 1 h, 70-100% yield; (iii) 3-bromo-N-(4-formylphenyl)-4-methoxybenzamide,[20] PTSA monohydrate, toluene, N_2, 150 °C, 5-8 h, 70-82% yield; (iv) $NaBH_4$, 3:1 CH_2Cl_2 dry/MeOH or THF dry, N_2, 0 °C to room temp, 15-23 h, 60-100% yield; (v) LiOH, 5:1 THF/H_2O, room temp, overnight, 51-100% yield; (vi) proper amino ester, EDCI, DMAP, DIPEA, THF dry or THF dry/DMF dry, N_2, room temp, overnight, 70-94% yield; (vii) (for derivative **14e**) piperidine 20% in DMF dry, N_2, room temp, 30 min, 100% yield.

Boronic acid derivatives **13d** and **14f** were synthesized according to Scheme 2. Coupling reaction of (4,4,5,5-tetramethyl-1,3,2-dioxaborolan-2-yl)methanaminium chloride with benzazole acid derivatives **9a,b** in the presence of 2-(1*H*-Benzotriazole-1-yl)-1,1,3,3-tetramethylaminium tetrafluoroborate (TBTU) and DIPEA gave boronic ester **27a,b**[26] that underwent to oxidative cleavage by use of sodium metaperiodate in the presence of NH_4OAc_{aq} 0.1 N, to furnish boronic acids **13d** and **14f**.[27]

Scheme 2. Synthetic Route to **13d** and **14f** Derivatives[a]

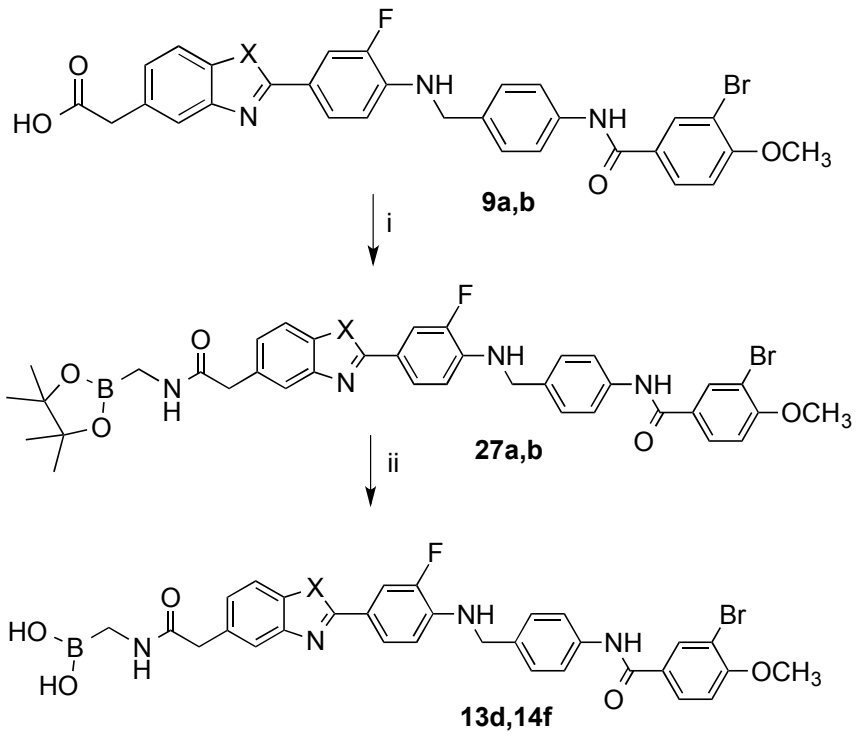

[a] Reagents and conditions: (i) (4,4,5,5-tetramethyl-1,3,2-dioxaborolan-2-yl)methanaminium chloride, TBTU, DIPEA, THF dry, N_2, -80 °C to room temp, 5 h, 75-82% yield; (ii) 0.1 N $NH_4OAc_{(aq)}$, $NaIO_4$, acetone, room temp, overnight, 35-38% yield.

Benzimidazole derivative **15** was obtained as reported in Scheme 3. *o*-Phenylendiamine and the commercially available 4-amino-3-fluorobenzoic acid have been reacted in the presence of polyphosphoric acid (PPA) to obtain compound **25**. The terminal amine of **25** was then condensed with 3-bromo-N-(4-formylphenyl)-4-methoxybenzamide[20] using acetic acid as a catalyst, to obtain the imine **26** that is in turn reduced using sodium borohydride, to give **15**.

Scheme 3. Synthetic Route to **15** Derivative[a]

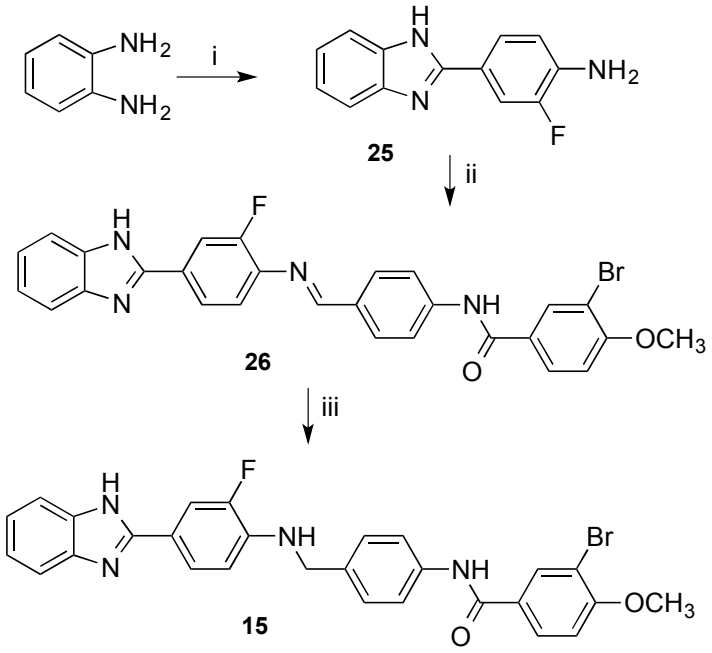

[a] Reagents and conditions: (i) PPA, 4-amino-3-fluorobenzoic acid, 220 °C, 5 h, 60% yield; (ii) 3-bromo-*N*-(4-formylphenyl)-4-methoxybenzamide[20], AcOH, 70 °C, 20 min, 60% yield; (iii) $NaBH_4$, DMF dry, room temp, 2 h, 70% yield.

The synthesis of benzoxazole compound **10c** is outlined in Scheme 4. The hydroxyaniline **28**[22] was acylated with acyl chloride **29**[28] using Et_3N as a base, to obtain the amide **30** that subsequently underwent to acid catalyzed ring closure, furnishing benzoxazole derivative **31**.

This compound has been condensed with aniline **32** using PTSA as catalyst, to give imine intermediate **33**[22] that was in turn reduced to the corresponding benzylamino compound **34** using sodium borohydride as reducing agent. Finally, the alkaline hydrolysis of **34** furnished the desired acid derivative **10c**.

Scheme 4. Synthetic Route to **10c** Derivative[a]

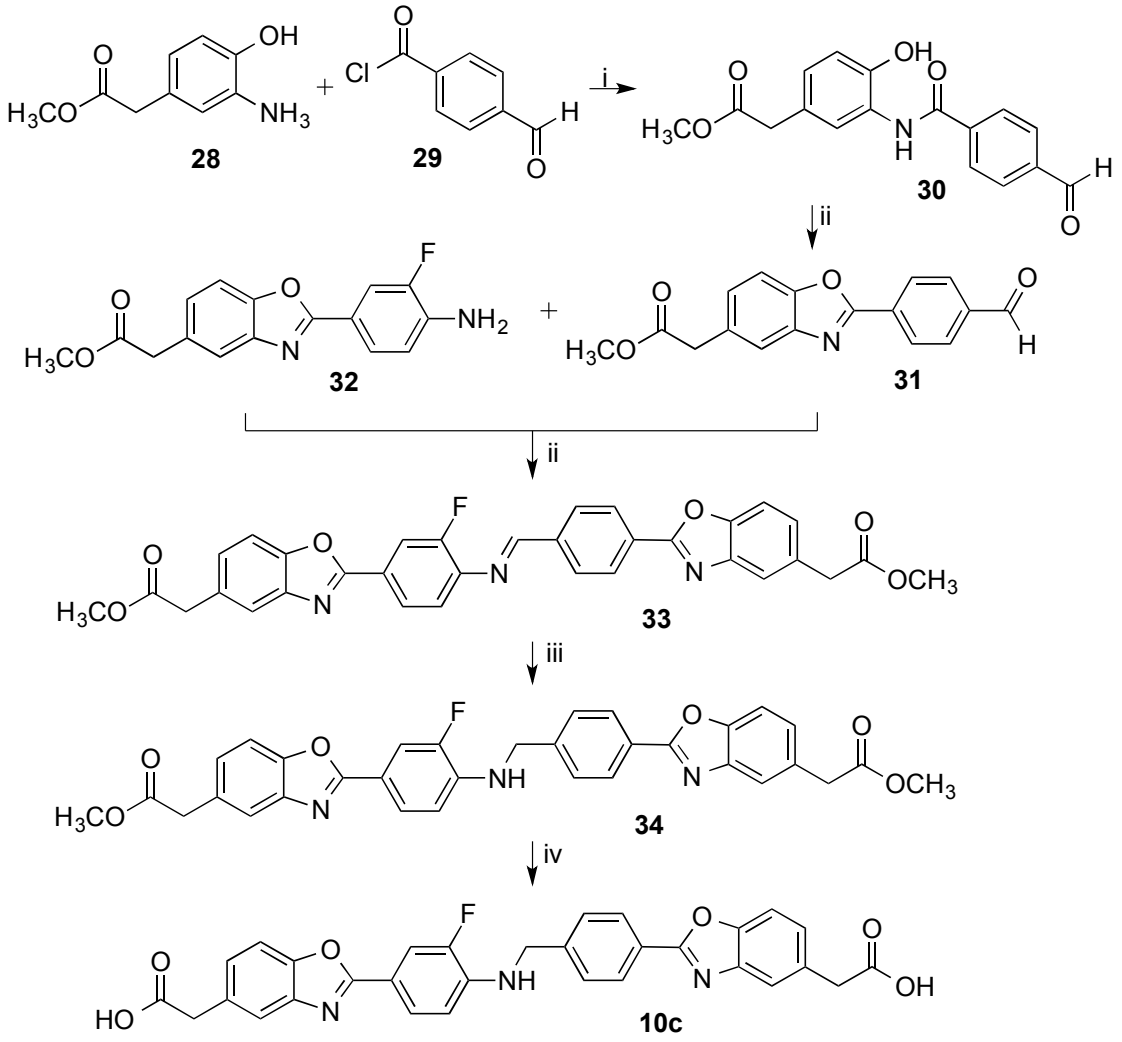

[a] Reagents and conditions: (i) Et_3N, CH_2Cl_2 dry, N_2, 0 °C to room temp, overnight, 73% yield; (ii) PTSA, toluene, 130 °C or 150 °C, 3-18 h, 37-87% yield; (iii) $NaBH_4$, 30:1 THF/H_2O, 0 °C to room temp, overnight, 26% yield; (iv) LiOH, 5:1 THF/H_2O, room temp, overnight, 68% yield.

Table 1. Hpse inhibitory activities of the newly synthesized **9a**,**b**, **10a-c**, **13a-d**, **14a-f**, **15** (Fondaparinux Hpse assay).

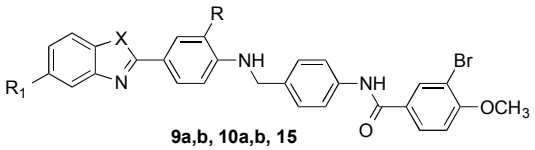

9a,b, 10a,b, 15

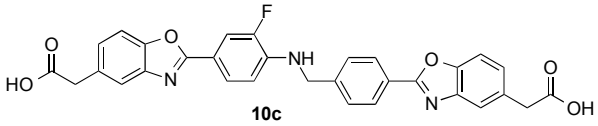

10c

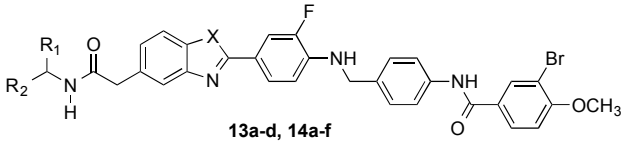

13a-d, 14a-f

Cpd	X	R	R_1	R_2	IC_{50}[a]	
					μM	μg/mL
9a	NH	F	CH_2COOH	-	2.86	1.73
9b	NH	H	CH_2COOH	-	>10	>5.8
10a	O	F	CH_2COOH	-	2.56	1.55
10b	O	H	CH_2COOH	-	>10	>5.8
10c	-	-	-	-	2.69	1.66
13a	NH	F	H	COOH	0.64	0.42
13b	NH	F	CH_3	COOH	3.46	2.33
13c	NH	F	CH_2Ph	COOH	1.59	1.19
13d	NH	F	H	$B(OH)_2$	1.19	0.78
14a	O	F	H	COOH	1.33	0.88
14b	O	F	CH_3	COOH	2.29	1.55
14c	O	F	CH_2Ph	COOH	5.70	4.28
14d	O	F	CH_2CH_2COOH	COOH	0.82	0.60
14e	O	F	$(CH_2)_4NH_2$	COOH	>10	>1.3

14f	O	F	H	$B(OH)_2$	> 10	> 6.6
15	NH	F	H	-	0.16	0.09
1					0.005	0.100
6					0.37	0.19

[a]Dose causing 50% inhibition of Hpse enzymatic activity as determined from dose response curves (mean of duplicates; SD always < 10%) repeated at least twice in separate experiments.

Evaluation of Biochemical Activities.

In Vitro Screening for Hpse Inhibitory Activity. All the newly synthesized compounds **9a,b, 10a-c, 13a-d, 14a-f,** and **15** were tested *in vitro* by the assay, originally developed by Hammond and coworkers based on the Hpse-mediated cleavage of the synthetic heparin fragment, the pentasaccharide Fondaparinux (AGA*IA), which corresponds to the methyl glycoside of the antithrombin III (ATIII)-activating pentasaccharide sequence of heparin.[29,30] The results for newly synthesized compounds, expressed as IC_{50} values generated from the dose-response curves, are reported in Table 1 together with those of reference compounds **1** and **6**.

Among the sixteen tested compounds, only 4 compounds (**9b**, **10b**, **14e,f**) resulted inactive (IC_{50} > 10 μM) whereas the majority of the newly synthesized compounds were moderately active, showing inhibitory potencies within the low micromolar-submicromolar range.

The acetic acid benzimidazolyl derivative **9a** and its benzoxazolyl counterpart **10a** proved to be able to reduce the enzymatic activity at similar low micromolar concentrations (IC_{50} values of 2.86 and 2.56 μM, respectively) suggesting that both scaffolds are effective in inhibiting Hpse. On the contrary, when the fluorine atom in *ortho* position of the amino group is replaced by the hydrogen one, an activity decrease was observed (compare **9a** with **9b** and **10a** with **10b**). Moreover, in order to better understand the role of the fluorine atom in inhibiting Hpse, derivative **6** lacking such atom in *ortho* position has been synthesized and tested. In our assay the

IC_{50} of compound **6** was 0.37 μM, while its fluorinated counterpart **15** resulted in an IC_{50} of 0.16 μM, thus showing an about 2-fold increase in the inhibitory potency. Taken together, these results suggest that the introduction of a fluorine atom improves the activity against the targeted enzyme.

Several structural modifications were carried on the acetic acid group of both benzimidazole and benzoxazole derivatives. Regarding the benzimidazole series, by removing the acetic acid group of compound **9a**, a higher than 17-fold gain in the inhibitory potency was observed, leading to the best active derivative among the newly synthesized ones (**15**, IC_{50} = 0.16 μM). Similarly, the functionalization of the acetic acid portion of **9a** with various amino acids led to derivatives **13a-c** endowed with higher potency than the parent compound, except for derivative **13b**. In fact, the activity decreases with the following order: Gly>Phe>Ala. More in detail, both the glycine (**13a**) and the phenylalanine (**13c**) derivatives showed better inhibitory profile than **9a**, with **13c** being 1.8 times more active than its acetic acid counterpart **9a** while **13a** reported a 4-fold increase in inhibiting the enzyme (**9a**, IC_{50} = 2.86 μM; **13a**, IC_{50} = 0.64 μM; **13c**, IC_{50} = 1.59 μM). Conversely, alanine derivative **13b** showed a slight decrease (IC_{50} = 3.46 μM), even though in the same order of magnitude of the enzymatic activity inhibition obtained with **9a**.

Regarding the benzoxazole series, the elongation of the acetic acid portion of **10a** led to amino acidic derivatives **14a-e**. As for benzimidazoles compounds, also in this case an activity gain with respect to their parent compound **10a** was observed. Indeed, glycine (**14a**), alanine (**14b**) and glutamate (**14d**) derivatives improved the inhibitory activity of **10a** of about 2, 1.2 and 3.2 times, respectively. It is worthy of note that the functionalization of the acetic acid group with a glutamate led to the best acting compound of the benzoxazole series (**14d**, IC_{50} = 0.82 μM). Differently, phenylalanine (**14c**) and lysine (**14e**) derivatives reported less encouraging results

than their acetic acid counterpart **10a**, with IC_{50} = 5.7 μM and IC_{50} > 10 μM, respectively. Thus, in the same fashion as for benzimidazole amino acids, it is possible to state that the activity decreases with the following order: Glu>Gly>Ala>Phe>Lys. In the view of the above, for both benzimidazoles and benzoxazoles derivatives, the amino acid conjugation seems to be a useful strategy to inhibit Hpse enzyme.

Furthermore, we investigated also the activity of groups that could mimic the glycine moiety through its replacement with an (aminomethyl)boronic acid group. In particular, we synthesized derivative **13d** as boronic acid counterpart of benzimidazole **13a** while compound **14f** represents the analogue of **14a**. For both boronic acids an activity loss was observed, being **14f** inactive (IC_{50} higher than 10 μM) and **13d** nearly 2-fold less active than the corresponding glycine derivative **13a** (**13d**, IC_{50} = 1.19 μM; **13a**, IC_{50} = 0.64 μM).

As mentioned above, we also synthesized and evaluated the pseudo-symmetric derivative **10c**, characterized by a second benzoxazole acetic group replacing the 3-bromo-4-methoxybenzamide moiety, that inhibited Hpse with an IC_{50} value of 2.69 μM, closely comparable to that of its analogue **10a** (IC_{50} = 2.56 μM). The similarity in their activity potencies allows speculating that this substitution may lead to the onset of additional favourable polar interactions of the second carboxylate with the hydrofilic substrate binding pocket of the targeted enzyme.

Molecular Modelling. Molecular docking studies were performed to identify the structural requisites responsible for Hpse inhibition. The crystal structures of human Hpse in complex with oligosaccharides provide fundamental insights into the architecture of the enzyme binding cleft. Two distinct subunits, referred to as N-terminal 8-kDa (residues Q36-E109) and C-terminal 50-kDa (residues K158-I543) chains, respectively, originate the mature Hpse heterodimer after

proteolytic activation of the proenzyme proheparanase. The substrate binding site is characterized by an elongated shape, with the catalytic residues E225 and E343 placed in the middle of a narrow channel. At one side the binding site is delimited by heparin binding domain 2 (HBD-2; residues 270 to 280).[31] The opposite extremity is widely open, pointing toward heparin binding domain 1 (HBD-1; residues 158 to 171) and toward a cavity, delimited by A388, N390 and G350, which accommodates the terminal iduronic acid of the glycosidic inhibitor dp4 in the crystal structure 5E9C (see Supporting Information, Figure S1).[32] The structure of Hpse from this complex was used to model the interaction between the enzyme and the benzazole derivatives. As the inhibitory potency of the compounds was tested on the catalytically active GS3 construct of human Hpse, in which the 8-kDa and 50-kDa chains are connected by a peptide linker (GS3),[33] we first built a model of the single-chain GS3 Hpse by adding the connecting peptide using MODELLER 9.16 software.[34] The structure of GS3 Hpse is depicted in Figure S1 in which the GS3 peptide is shown. The connecting peptide GS3 did not interact with amino acids of the co-crystallized ligand dp4. This model of GS3 Hpse was used for molecular docking studies to devise a putative binding mode of benzazole inhibitors.

Docking solutions obtained with Glide 3.9[35,36] showed a common interaction scheme for compounds carrying a carboxylic group. The inhibitors lie within the substrate binding cleft and occupy the catalytic site, bending in correspondence of their benzylamine portion and surrounding the glycine loop of Hpse involved in substrate recognition. The acidic portions of benzazole derivatives interact with a polar region which includes HBD-2 and extends to its surroundings. In particular, salt bridges or hydrogen bonds are formed with Q270 and R272 of HBD-2, while some compounds also interact with the side chain of N227.

The best poses obtained for ~~the~~ compounds **9a** and **10a** are depicted in Figure 3. Inhibitors assume a similar binding mode, accommodating the benzimidazole or benzoxazole ring within the substrate binding site in proximity of the catalytic residues and placing the *N*-phenylbenzamide moiety within a wide cleft lined by residues G349, G350, A388, N390 and Y391. The ligands do not interact with the GS3 fragment built by homology modeling. The region occupied by the two compounds is superposable to that of the co-crystallized inhibitor dp4 (Figure 3, left), and their carboxylate group interacts with Q270 and R272 from HBD2 which are also the binding partners of the terminal sulfate group of inhibitor dp4. The benzimidazole NH undertakes a hydrogen bond with catalytic E343. The benzamide portion assumes a different conformation in the two compounds, allowing the formation of a hydrogen bond between the amide NH and the backbone oxygen of G350 in the case of **9a**, while the methoxy substituent of **10a** interacts with N390 (Figure 3, right). Overall, the compounds interact with relevant amino acids of the substrate binding site, comprising the catalytic glutamates and the glycine loop (G349 and G350) which constitutes the recognition site for the carboxylic group of the substrate glucuronic acid, likely impeding the interaction of heparan sulfate with the catalytic site.

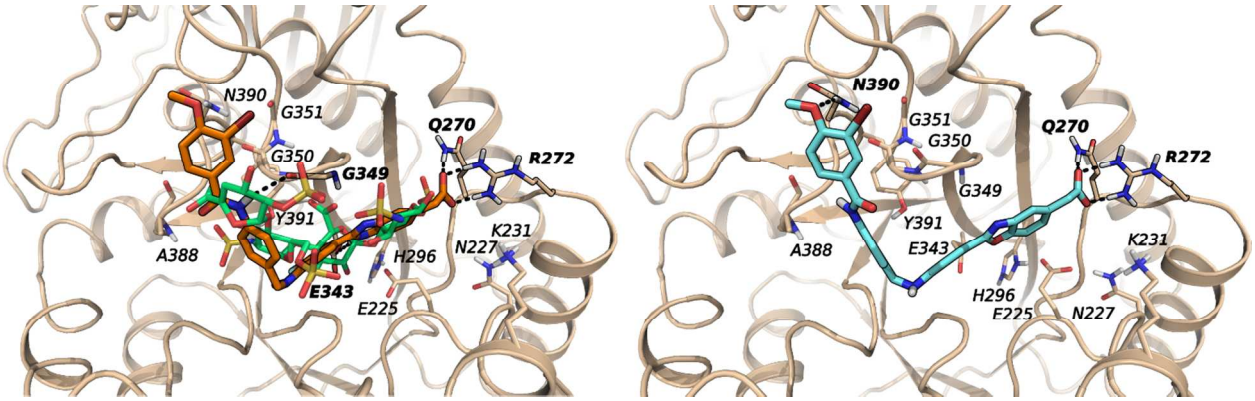

Figure 3. Binding mode of compounds **9a** and **10a** to Hpse. Left panel. Best docking pose for **9a** (orange carbons), superposed to the co-crystallized inhibitor dp4 (PDB 5E9C, green carbons). Right panel. Best docking pose obtained for **10a**.

To account for the effect of amino acid conjugation, docking studies were performed for the conjugated derivatives of inhibitors **9a** and **10a**, i.e., for compounds **13a-c** and **14a-e**. The best pose obtained for the most potent benzimidazole derivative (**13a**, conjugation with glycine) is depicted in Figure 4 (left). HBD-2 appears as the major anchoring point for the conjugated amino acids. The carboxylate group of **13a** interacts with the same Q270 and R272 bound to the unconjugated **9a**, while the two carboxylates of **14d** are hydrogen-bonded to R272 and N227. The presence of the linking amide group, absent in the unconjugated inhibitors, allows the formation of additional interactions with the substrate binding site, in particular with the catalytic E225. Amino acid conjugation produces a shift of the benzimidazole within the active site, and its NH group interacts with the side chain of Y391, another amino acid involved in substrate recognition. The benzamide portion occupies the cleft lined by residues G350, A388, N390 and Y391 forming hydrogen bonds with polar amino acids. Generally, docking solutions for compounds **13b-c** and **14a-c** showed arrangements similar to that described for **13a**, which is consistent with the steric tolerance of Hpse for conjugated structures. The amino acid side chains were sterically tolerated, even if hydrophobic residues could not take additional interactions. Thus, the lower potency observed for the phenylalanine derivative **13c** compared with the glycine derivative **13a** might be due to the polar nature of the region surrounding the inhibitor surface (Supporting Information, Figure S2). No quantitative relationship was found between inhibitory potency and the scoring function, which estimates the interaction energy (GScore, see Supporting Information Table S1), as expected by the limited range of potency variation among the active compounds.

Compound **14d** (the benzoxazole derivative conjugated with glutamic acid) lies in the same region and undertakes polar interactions with A388 and K491, but its amino acid portion shows a peculiar arrangement, binding Q270 and R272 through its side-chain carboxylate, while taking additional interactions between its main-chain carboxylate and the polar portions of N227 and K231 (Figure 4, right). Qualitatively, this is consistent with its high inhibitory potency.

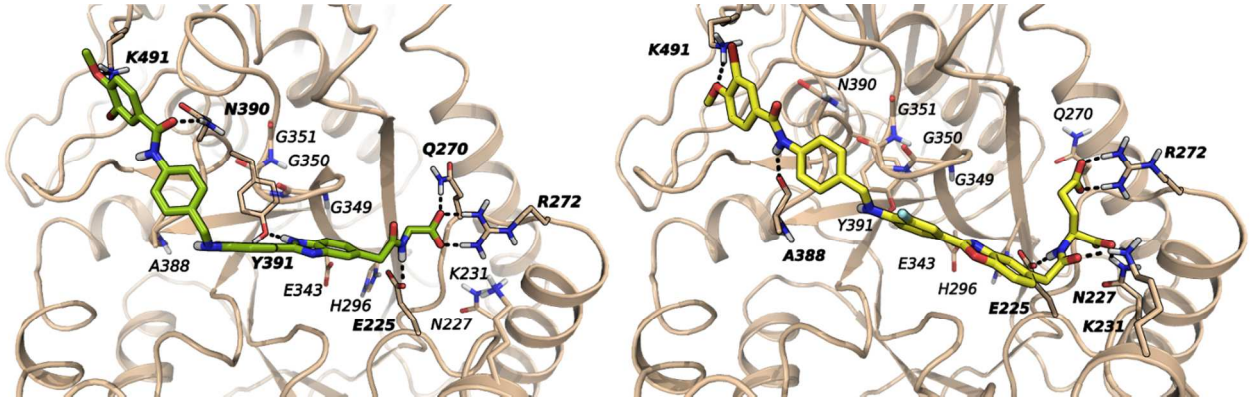

Figure 4. Docking poses obtained for **13a** (left panel) and **14d** (right panel).

The inactive derivative **14e** gave no high-score solution with the same orientation. This is likely due to its positive charge which is responsible for electrostatic repulsion with basic residues of the HBD-2 region.

The Hpse-inhibitor complexes obtained for compounds **9a**, **10a**, **13a** and **14d** were stable during 25 ns of molecular dynamics simulation, with the inhibitors accommodated within the substrate binding cleft and maintaining a stable network of polar interactions. Fluctuations of the root mean square deviation (RMSD) of the ligand heavy atoms is mainly due to the mobility the of 3-bromo-4-methoxy-*N*-phenylbenzamide group, while the benzimidazole and benzoxazole portions remain in close contact with the active site, and the terminal acidic groups maintain the

network of polar interactions with residues of the HBD-2 region (see Supporting Information, Figure S3). Analysis of the trajectories revealed that the hydrogen bonds formed by the benzimidazole NH groups of **9a** and **13a** are not maintained during the simulations, suggesting that this interaction is accessory and not strong enough to provide higher potencies compared to the benzoxazole derivatives.

Evaluation of Biological Activities

Proliferation Assay. Upon screening as inhibitors of Hpse activity, four of the most active Hpse inhibitors (**13a**, **14a**, **14d** and **15**) were further characterized in vitro by a cell proliferation assay to assess their effect on the growth of three human tumor cell lines, namely HT1080 (fibrosarcoma), U2OS (osteosarcoma) and U87MG (glioma) expressing different levels of Hpse[37-39] using **6** as the reference compound. Cells were treated for 72 hours with serial dilutions (covering the active concentrations in the Hpse enzyme assay) of each test compound as well as of the two not branched benzimidazoles: the reference compound **6** and its fluoro derivative **15**. As determined by cell proliferation curves (data not shown), none of the newly synthesized benzazoles, **13a**, **14a** and **14d** showed antiproliferative activity up to 2.5 μM, the maximum concentration assessed. On the contrary, in the same assay, the reference compound **6** and its derivative **15** moderately inhibited proliferation of the three cell lines (IC_{50} values between 1.7 and 8.7 μM) (Table 2).

Table 2. Proliferation assay on the newly synthesized benzazoles **13a**, **14a**, **14d**, **15** and reference compound **6**

compd	IC_{50} (μM)[a]		
	cell line		
	HT1080	U87MG	U2OS
13a	NA	NA	NA
14a	NA	NA	NA
14d	NA	NA	NA
15	8.7	2.8	1.7
6	3.1	2.7	2.1

Antiproliferative activity of compounds tested on HT1080, U87MG and U2OS tumor cells upon 3 days of treatment. [a]IC_{50} values (μM; SD always < 10%) determined from dose response curves (each concentration tested in duplicate) repeated at least twice in separate experiments. NA: not active.

Invasion assay. It is known that Hpse has a pivotal role in promoting cancer cell invasion and metastasis. Thus, we tested the most active compounds in enzyme assay (**13a**, **14d** and **15**) in the Matrigel cell invasion assay with HT1080, U87MG and U2OS cells using compound **6** as the reference compound. All the compounds were assessed at not toxic concentrations. More in details, compounds **6** and **15**, were tested at concentrations below the relative IC_{10} values measured for each cell line (according to data of anti-proliferative assays) whereas the other ones were tested at 10 μM.

Compound **15** was able to markedly inhibit the invasion potential of all three tumor cell lines, similarly to the reference compound **6**, whereas derivative **14d** was active against HT1080 and U87MG cells but was ineffective against U2OS cells.

Table 3. Inhibition of invasive potential of HT1080, U87MG and U2OS human cell lines by derivatives **13a**, **14d** and **15** and reference compound **6**

compd	Conc. tested	HT1080	U87MG	U2OS
13a	10 μM	-	-	+
14d	10 μM	++	++	-
15	1 μM	++	++	++
6	1 μM	++	++	++

Matrigel cell invasion assay on HT1080, U87MG and U2OS tumor cells upon 24 hours of treatment. Score symbols: "-"no inhibition; "+" < 50% inhibition; "++" 50-90% of inhibition of cell invasion, with respect to invading cells in the absence of drugs.

Compound **15** was further investigated on two soft tissue sarcoma cell lines, i.e the human synovial sarcoma cell line CME-1 and the rhabdoid tumor cell line A204, known to express high levels of Hpse at a comparable extent (not shown). Treatment with heparin derivatives, Hpse inhibitors, has been previously reported to heavily affect behaviors associated with the malignant phenotype of these two sarcoma cell lines.[11,39,40] As shown in Figure 5A, **15** inhibited cell growth of both sarcoma cell lines displaying IC_{50}s similar to those measured on other tumor cell lines (Table 2).

Although cell cytotoxicity could influence the Matrigel invasion results, the anti-invasive effect we observed was not substantially affected by the drug antiproliferative activity. Compound **15** concentrations used in the invasion assay with CME-1 and A204 cells were nearby the IC_{50}s evaluated after 72 h of drug treatment. However, in the Matrigel invasion assay, cells were exposed to the drug for 24 h then counted before transfer into the Transwell chambers. Compound **15** (1.5 μM) for 24h does not influence proliferation of both A204 and CME-1 cells.

The drug slightly affects cell growth after 24h of exposure inducing an inhibition of proliferation around 5% in A204 cells and 15% in CME-1 at 3.1 μM.

In addition, compound **15** inhibited Matrigel invasion by both sarcoma cell lines in a dose-dependent way (Figure 5 B, C). Overall, these findings evidenced the ability of the Hpse inhibitor **15** to inhibit proliferation and invasion potential of tumor cells of different origin.

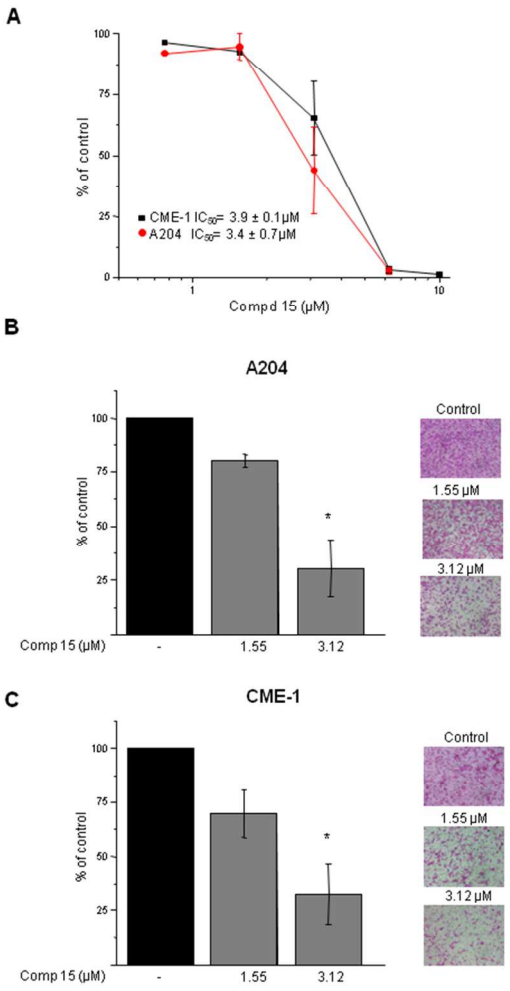

Figure 5. Compound **15** inhibited proliferation and invasion of human sarcoma cells. A) The day after seeding, cells were treated with the indicated drug concentrations. After 72h, the drug

antiproliferative effect was assessed by cell counting. Curves are from one representative experiment out of two, performed in duplicate. Data represent mean percentage values ± SE. IC_{50}s, mean values ± SD from two independent experiments. B) A204 and C) CME-1 cells pretreated with the compound at the indicated concentrations were transferred to Matrigel-coated Transwell chambers and incubated for additional 24h. Columns represent mean percentage values ± SE of at least three independent.*P<0.05 Representative images of filters are shown. Original magnification 100X.

Effects on gene expression. It has been reported that a fraction of active Hpse is translocated into the cell nucleus where, upon degradation of the nuclear heparan sulfate, contributes in regulating transcription of multiple genes that drive an aggressive tumor phenotype.[41,42] Therefore, we wondered if our selected Hpse inhibitors are also able to affect gene expression. To this aim, HT1080 cells were treated for 24 hours with derivative **15** as compared to the reference compound **6,** both at 1.0 μM concentration. Then, the mRNA levels related to genes encoding for proangiogenic factors, such as FGF1/2, VEGF, MMP-9, and for Hpse (HPSE-1) were measured by a quantitative Real-Time PCR assay. Results highlighted a relevant inhibitory effect of **15** with respect to transcription of MMP-9 gene and a moderate effect on transcription of all the other genes assessed (Figure 6). Instead, compound **6** was only able to inhibit moderately the expression of VEGF and MMP9 genes but had no effect on FGF-1, FGF-2 and HPSE-1 expression.

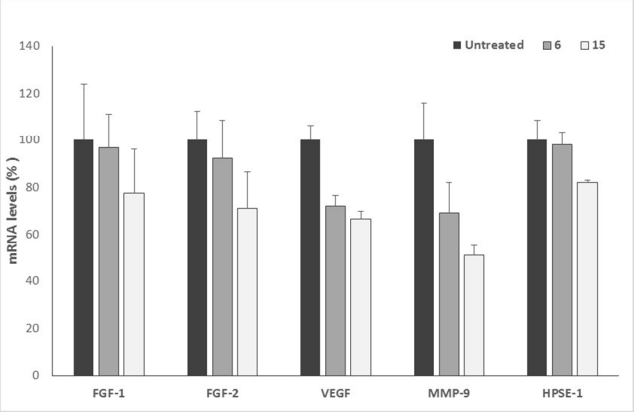

Figure 6. Effect of compounds **6** and **15** on the expression of selected genes**.** The expression levels of FGF-1, FGF-2, VEGF, MMP-9 and HSPE-1 mRNA in HT1080 cells, upon 24 h of treatment, were measured through real-time qPCR analysis. Results are expressed as percent with respect untreated cells.

Conclusions

The increasing demand of new and more effective anticancer strategies presses the research of innovative, steadfast and easily druggable targets. ECM degrading enzymes involved in tumor onset and progression are attractive targets in cancer therapy. Among them, a promising target enzyme is the *endo*-β-D-glucuronidase, Hpse. Hpse plays a major role in the onset of several human both metabolic and inflammatory diseases and, notably, up-regulation of Hpse is associated with increased tumor size, tumor angiogenesis, enhanced metastasis and poor prognosis in various solid and hematological malignancies. Preclinically, Hpse has been demonstrated to be an attractive and druggable target for innovative therapeutic approaches. In this study, we reported the design, synthesis and biological evaluation of new benzimidazole and benzoxazole derivatives as Hpse inhibitors. The majority of the newly synthesized compounds showed potencies within the low micromolar-submicromolar range when tested in Hpse

enzymatic assay. The benzimidazole derivative **15 (SST0623AA1)** proved to be the best inhibitor with IC_{50} of 0.16 μM, 2-fold higher than that of its non-fluorinated counterpart **6**. Furthermore, the amino acid derivatives **13a** and **14d** displayed inhibitory potency in the same order of magnitude of **15**, (IC_{50} of 0.64 and 0.82 μM respectively). These two most potent amino acid conjugates **13a** and **14d** along with the corresponding unconjugated derivatives **9a** and **10a** were also evaluated through docking studies into crystallized human Hpse to rationalize their enzymatic activity and propose a binding mode consistent with their activity. The investigated compounds appeared to interact with relevant amino acids of the catalytic site thus impeding the accommodation of the substrate within the active site. The *in silico* studies confirmed also our hypotheses according to which the amino acid conjugation seems to be useful for the enzymatic inhibition and that both benzazolyl scaffolds are effective in inhibiting Hpse. The best-acting compounds of both the amino acid conjugated and unconjugated series in enzymatic assay (**13a**, **14a,d**) do not affect cell proliferation up to 2.5 μM. Very importantly, invasion assay confirmed the anti-metastatic potential of compounds **14d** and **15**. Consistent with its ability to inhibit Hpse, likely resulting also in degradation of the nuclear heparan sulfate that it is known to affect the control of gene transcription, compound **15** is also able to inhibit the transcription of genes encoding for proangiogenic factors such as MMP-9, VEGF and FGFs in tumor cells, although a mechanism of inhibition not depending on the enzymatic activity of HPSE cannot be excluded.

In conclusion, in this study we provided new insights for future development of new small molecules as effective Hpse inhibitors. Further optmization of our best promising derivatives **13a**, **14d** and **15** might lead to a more effective modulation of Hpse enzymatic activity, thus actively contributing to improve the therapeutic tools for those clinical indications in which Hpse proved to be a useful pharmacological target, including the antimetastatic effect.

Experimental section

Chemistry: General. Melting points were determined on a Bobby Stuart Scientific SMP1 melting point apparatus and are uncorrected. Compounds purity were always >95% determined by high pressure liquid chromatography (HPLC). HPLC analysis were carried out with a Shimadzu LC-10AD VP CTO-10AC VP. Column used was generally Discovery Bio Wide Pore C18 and C8 (10 cm × 4.6 mm, 3 μm) or Phenomenex Gemini C6-Phenyl (150 cm × 4.6 mm, 3 μm). IR spectra were recorded on a PerkinElmer Spectrum-One spectrophotometer. ^{1}H NMR spectra were recorded at 400 MHz on a Bruker AC 400 Ultrashield 10 spectrophotometer (400 MHz). Dimethyl sulfoxide-d_6 99.9% (CAS 2206-27-1), deuterochloroform 98.8% (CAS 865-49-6) and *N*,*N*-Dimethylformamide-d_7 (CAS 4472-41-7) of isotopic purity (Aldrich) were used. Mass spectra were recorded on a ThermoFinnigan LCQ Classic LC/MS/MS ion trap equipped with an ESI source and a syringe pump. Samples (10^{-4}-10^{-5} M in MeOH/H_2O 90:10) were infused in the electrospray system at a flow rate of 5-10 μL min^{-1}. When necessary, 50 μL of 10^{-2} M HCOOH or 10^{-2} M NH_3 were added to the sample solution, in order to promote the analyte ionization. Column chromatographies were performed on silica gel (Merck; 70−230 mesh). All compounds were routinely checked on TLC by using aluminum-baked silica gel plates (Fluka DC-Alufolien Kieselgel 60 F_{254}). Developed plates were visualized by UV light. Solvents were reagent grade and, when necessary, were purified and dried by standard methods. Concentration of solutions after reactions and extractions involved the use of rotary evaporator (Büchi) operating at a reduced pressure (ca. 20 Torr). Organic solutions were dried over anhydrous sodium sulfate (Merck). All solvents were freshly distilled under nitrogen and stored over

molecular sieves for at least 3 h prior to use. Analytical results agreed to within ±0.40% of the theoretical values.

General procedure A (GP-A) to obtain Acetic Acid Derivatives (9a,b, 10a-c, 13a-c and 14a-e): A solution of LiOH (2.5 mmol) in distilled water was added to a solution of the appropriate ester (1 mmol) in THF (fivefold the water amount) and the reaction was stirred vigorously overnight. The organic phase was removed under vacuum and the resulting suspension was acidified with 1N HCl until pH 4-5 was obtained. The solid formed was collected by filtration, then washed with water and dried under IR lamp to afford pure acids. For each compound amount of ester derivative; THF; R_f; yield (%); melting point (°C); recrystallization solvent; IR; ^{1}H NMR and MS (ESI) are reported.

General procedure B (GP-B) to obtain Amino Ester Derivatives (11a-c and 12a-e): Amino ester hydrochloride (1.2 mmol), EDCI (1.2 mmol), DMAP (1.2 mmol) and DIPEA (2.4 mmol) were added to a well-stirred solution of acid derivative (1 mmol) in *dry* THF (for derivatives **12a-e**) or in a mixture of *dry* THF/*dry* DMF (for derivatives **11a-c**). The mixture was stirred at room temperature overnight under argon atmosphere. The organic phase was removed under vacuum and the crude was treated with water. The solid formed was filtered, washed with water and dried under IR lamp to afford the pure amide derivatives. For each compound amount of amino ester hydrochloride; volume of solvent; R_f; yield (%); melting point (°C); recrystallization solvent; IR; ^{1}H NMR and MS (ESI) are reported.

General procedure C (GP-C) to obtain Boronic Acid Derivatives (13d and 14f): To a stirred solution of the boronate ester (1 mmol) in the proper solvent, NH_4OAc_{aq} (23 mL, 0.1 N) and $NaIO_4$ (2.2 mmol) was added, following a known procedure.[27] The mixture was stirred vigorously at room temperature overnight. Acetone was removed under vacuum and the resulting

solid was collected by filtration, washed with water and dried under IR lamp prior to be washed diethyl ether, affording pure boronic acid derivatives. For each compound amount of boronic ester derivative; R_f; yield (%); melting point (°C); recrystallization solvent; IR; ^{1}H NMR and MS (ESI) are reported.

General procedure D (GP-D) to obtain Nitrobenzimidazole Derivatives (17a,b): Ceric ammonium nitrate (0.1mmol) was added into a well-stirred solution of **16** (1mmol), the proper aldehyde (1mmol) and H_2O_2 30% (4mmol) in *dry* acetonitrile (3 mL) and the mixture was stirred at 50° C for 50 minutes under argon atmosphere, according to a known procedure.[24] The reaction was cooled to room temperature, quenched with water and the organic phase was evaporated under vacuum. The precipitate that formed was filtered and washed with water, AcOEt, petroleum ether and dried under IR lamp to afford the pure nitrobenzimidazole. For each compound amount of the proper aldehyde; R_f; yield (%); melting point (°C); IR;^{1}H NMR and MS (ESI) are reported.

General procedure E (GP-E) to obtain Benzimidazole Amine Derivatives (18a,b): $NHEt_2$ (1mmol), Pd/C 10% (10% w/w) and ammonium formate (10 mmol) were added to a well-stirred solution of the nitroderivative (1 mmol) in the proper solvent, and it was refluxed for 1h under nitrogen atmosphere. The reaction was quenched with water, cooled to room temperature, filtered on Celite and washed with AcOEt. The organic layer was evaporated under vacuum and the raw material was extracted with AcOEt and water. The organic phase was separated, washed with brine, dried over sodium sulphate, filtered and evaporated under vacuum to afford the pure amine. For each compound amount of nitro derivative; volume of solvent; R_f; yield (%); melting point (°C); IR; ^{1}H NMR; and MS (ESI) are reported**.**

General procedure F (GP-F) to obtain Imine Derivatives (20a,b, 21a,b and 33): A well-stirred suspension of the opportune amine (1mmol), 3-bromo-*N*-(4-formylphenyl)-4-methoxybenzamide[20] (1mmol) or methyl 2-(2-(4-amino-3-fluorophenyl)benzo[d]oxazol-5-yl)acetate **32**[22] (1mmol) (for derivative **33**) and PTSA monohydrate (0.01 mmol) in toluene (25 mL) was stirred at 150° C for 5-18 h. Water which formed was removed by the means of Dean-Stark apparatus. The yellow solid that formed was filtered, washed with warm toluene and hexane and dried under IR lamp to afford the pure imine derivative. For each compound amount of amino derivative; R_f; yield (%); melting point (°C); IR; ^{1}H NMR and MS (ESI) are reported.

General procedure G (GP-G) to obtain Benzylamino Derivatives: (22a,b, 23a,b and 34)

$NaBH_4$ (2.58 mmol) was added into a well-stirred solution of the appropriate imine (1 mmol) refrigerated in an ice-bath in *dry* THF (for derivatives **22a,b**) or in 3:1 CH_2Cl_2/MeOH (for derivatives **23a,b**) or in 30:1 THF/H_2O (for derivative **34**). The reaction, periodically checked by ^{1}HNMR, was stirred at room temperature under argon atmosphere and further amounts of $NaBH_4$ were added portion wise within 15-23 hours, in order to induce completion of reaction. The organic phase was removed under vacuum and the raw material was treated with water. The solid formed was filtered, washed with water, petroleum ether and dried under IR lamp to afford the pure benzylamino derivative. For each compound amount of imine derivative; volume of solvent; additional amounts of $NaBH_4$ and period of addition; R_f; yield (%); melting point (°C); recrystallization solvent; IR; ^{1}H NMR and MS (ESI) are reported.

General procedure H (GP-H) to obtain Boronic Ester Derivatives (27a,b): (4,4,5,5-tetramethyl-1,3,2-dioxaborolan-2-yl)methanaminium chloride (1.2 mmol), **9a,b** (1 mmol), and TBTU (1.4 mmol) were solubilized in *dry* THF (45 mL), and the mixture was cooled to -80° C while stirring. After that a solution of i-Pr_2NEt (3.6 mmol) in *dry* THF (6 mL) was added

dropwise during 2 h to a stirred reaction mixture maintaining the temperature at -80°C. The mixture was stirred for another 1.5 h, and then slowly heated to room temperature, as previously reported in literature.[26] The solvent was removed under vacuum and the crude was treated with distilled water, the solid formed was filtered, washed with water and dried under IR lamp to afford the pure boronic ester derivatives. For each compound amount of acetic acid derivative; R_f; yield (%); melting point (°C); recrystallization solvent; IR; ^{1}H NMR and MS (ESI) are reported.

2-(2-(4-((4-(3-bromo-4-methoxybenzamido)benzyl)amino)-3-fluorophenyl)-1*H*-benzo[*d*]imidazol-5-yl)acetic acid (9a). Compound **9a** was prepared from **22a** by means of GP-A. **22a** (1.06 g, 1.7mmol); 20mL; R_f (AcOEt: MeOH 3:2): 0.32; 100% as a yellow solid; 180-183°C; isopropanol; IR *v* 3299 (NH benzylamine), 2937 (OH), 1722 (C=O acid) cm^{-1};^{1}H NMR (DMSO d_6) δ 3.71 (s, 2H, CH_2 acetic), 3.93 (s, 3H, OCH_3), 4.45 (bd, 2H, CH_2benzylamine), 6.80 (bt, 1H, NH benzylamine), 7.03-8.21 (m, 13H, Ar), 10.18 (s, 1H, amide), 12.34 (bs, 1H, benzimidazole), 14.00 (bs, 1H, OH); MS: m/z (ESI) calcd for $[C_{30}H_{24}BrFN_4O_4]^+$: 602.10, found: 603.

2-(2-(4-((4-(3-bromo-4-methoxybenzamido)benzyl)amino)-phenyl)-1*H*-benzo[*d*]imidazol-5-yl)acetic acid (9b). Compound **9b** was prepared from **22b** by means of GP-A. **22b** (0.13 g, 0.22 mmol); 3 mL; R_f (AcOEt: MeOH 4:1): 0.18; 82% as a yellow solid; 283-286°C; isopropanol; IR *v* 3285 (NH benzylamine), 2940 (OH), 1711 (C=O acid) cm^{-1}; ^{1}H NMR (DMSO d_6) δ 3.72 (s, 2H, CH_2acetic), 3.93 (s, 3H, OCH_3), 4.37 (bd, 2H, CH_2benzylamine), 6.79 (m, 2H, NH benzylamine and 1H Ar), 7.23-8.22 (m, 13H, Ar), 10.19 (s, 1H, amide), 12.35 (bs, 1H, benzimidazole), 14.00 (bs, 1H, OH); MS: m/z (ESI) calcd for $[C_{30}H_{25}BrN_4O_4]^+$: 584.11, found: 585.

2-(2-(4-((4-(3-bromo-4-methoxybenzamido)benzyl)amino)-3-fluorophenyl)benzo[d]oxazol-5-yl)acetic acid (10a). Compound **10a** was prepared from **23a** by means of GP-A. **23a** (0.48 g, 0.77 mmol); 17.7 mL; R_f (n-hexane/ethyl acetate 1:1): 0.5; 100% as a yellow solid; 238 °C; washed with diethyl ether ; IR ν 3375 (NH) 1732 (C=O ester), 1650 (C=O amine) cm^{-1}; ^1H NMR (DMSO d_6) δ 3.63 (s, 3H, $COOCH_3$), 3.81 (s, 2H, $OCOCH_2$), 3.93 (s, 3H, OCH_3), 4.44 (br d, 2H, $NHCH_2$), 6.76 (t, 1H, benzene H, J = 8 Hz), 7.13 (br t, 1H, $NHCH_2$), 7.24 (t, 2H, benzoxazole C6-H and C4-H, J = 8 Hz), 7.36 (d, 2H, benzene H, J = 8 Hz), 7.59 (s, 1H, benzoxazole C4-H), 7.63 (d, 1H, benzoxazole C7-H,, J = 8 Hz), 7.70-7.80 (m, 4H, benzene H), 8.00 (br d, 1H, benzene H), 8.22 (s, 1H, benzene H), 10.18 (s, 1H, NHCO); MS: m/z (ESI) calcd for $[C_{30}H_{23}BrFN_3O_5]^+$: 603.08, found: 604.

2-(2-(4-((4-(3-bromo-4-methoxybenzamido)benzyl)amino)phenyl)benzo[d]oxazol-5-yl)acetic acid (10b). Compound **10b** was prepared from **23b** by means of GP-A. **23b** (0.2 g, 0.33 mmol); 8.8 mL; R_f (ethyl acetate): 0.6; 88% as a yellow solid; 249-250 °C; washed with diethyl ether; IR ν 3286 (OH), 1708 (C=O acid), 1636 (C=O amine) cm^{-1}; ^1H NMR (DMSO d_6) δ 3.60 (s, 2H, $OCOCH_2$), 3.94 (s, 3H, OCH_3), 4.36 (br d, 2H, $NHCH_2$), 6.75 (d, 2H, benzene H, J = 8 Hz), 7.11 (br t, 1H, $NHCH_2$), 7.18 (d, 1H, benzoxazole C6-H, J = 8 Hz), 7.25 (d, 1H, benzene H, J = 8 Hz), 7.35 (d, 2H, benzene H, J = 8 Hz), 7.52 (s, 1H, benzoxazole C4-H), 7.56 (d, 1H, benzoxazole C7-H, J = 8 Hz), 7.72 (d, 2H, benzene H, J = 8 Hz), 7.89 (d, 2H, benzene H, J = 8 Hz), 8.01 (d, 1H, benzene H, J = 8 Hz), 8.22 (s, 1H, benzene H), 10.19 (s, 1H, NHCO), 12.10 (br s, 1H, COOH); MS: m/z (ESI) calcd for $[C_{30}H_{24}BrN_3O_5]^+$: 585.09, found: 586.02.

2-(2-(4-(((4-(5-(carboxymethyl)benzo[d]oxazol-2-yl)-2-fluorophenyl)amino)methyl)phenyl)benzo[d]oxazol-5-yl)acetic acid (10c). Compound **10c** was prepared from **34** by means of GP-A. **10c** (0.4 g, 0.69 mmol); 30 mL; R_f

(chloroform/methanol 1:1): 0.37; 68% as a yellow-orange solid; 300°C dec.; DMF; IR ν 3387 (OH acid), 1623 (C=O acid) cm^{-1}; ^1H NMR (CH_3OD d_3) δ 3.52 (s, 3H, CH_3), 3.54 (s, 3H, CH_3), 4.55 (s, 4H, CH_2), 6.61 (t, 1H, J=8.4 Hz, benzene H), 7.22 (d, 1H, J=8.8 Hz, C6-H benzoxazole), 7.30 (d, 1H, J=8.8 Hz, C6-H benzoxazole), 7.41 (d, 1H, J=8.4 Hz, C7-H benzoxazole), 7.48-7.55 (m, 4H, C4-H benzoxazole, C7-H benzoxazole and benzene H), 7.60 (s, 1H, C4-H benzoxazole), 7.70-7.75 (m, 2H, C7-H benzoxazole and benzene H), 8.13 (d, 2H, J=7.2 Hz, benzene H). 96.80%; MS: m/z (ESI) calcd for $[C_{31}H_{22}FN_3O_6]^-$: 551.15, found: 549.80.

Ethyl 2-(2-(2-(4-((4-(3-bromo-4-methoxybenzamido)benzyl)amino)-3-fluorophenyl)-1*H*-benzo[*d*]imidazol-5-yl)acetamido)acetate (11a). Compound **11a** was prepared from **9a** by means of GP-B. Glycine ethyl ester hydrochloride (0.056g, 0.40 mmol); *dry* THF/*dry* DMF (35 mL:6 mL); 0.63 (AcOEt/MeOH 4:1); 80% as a yellow solid; 160-163°C; ethyl acetate; IR *v* 3273 (NH), 1736 (C=O), 1626, 1600 (C=O amide) cm^{-1}; ^1H NMR (DMSO d_6) δ 1.16 (t, 3H, CH_3CH_2O, J= 4 Hz), 3.54-3.56 (m, 2H, CH_2acetic), 3.81 (d, 2H, CH_2Gly, J=4 Hz), 3.93 (s, 3H, OCH_3), 4.06 (q, 2H, CH_3CH_2O, J=4Hz), 4.41 (bd, 2H, CH_2benzylamine), 6.71 (bt, 1H, NH benzylamine), 7.02-8.43 (m, 13H, Ar), 10.17 (s, 1H, amide), 12.46 (bs, 1H, benzimidazole); MS: m/z (ESI) calcd for $[C_{34}H_{31}BrFN_5O_5]^+$: 687.15, found: 688.

Ethyl 2-(2-(2-(4-((4-(3-bromo-4-methoxybenzamido)benzyl)amino)-3-fluorophenyl)-1*H*-benzo[*d*]imidazol-5-yl)acetamido)propanoate (11b). Compound **11b** was prepared from **9a** by means of GP-B. Alanine ethyl ester hydrochloride (0.092 g, 0.60 mmol); *dry* THF/*dry* DMF (50mL:3mL), R_f (AcOEt/MeOH 4:1) 0.55; 88.3% as a white-yellow solid; 145-148°C; ethyl acetate; IR *v* 3276 (NH), 1732 (C=O ester), 1647, 1626 (C=O amide) cm^{-1}; ^1H NMR (DMSO d_6) δ 1.14 (t, 3H, CH_3CH_2O, J= 4 Hz), 1.28 (d, 3H, CH_3 Ala, J=8Hz), 3.51-3.53 (m, 2H, CH_2acetic), 3.93 (s, 3H, OCH_3), 4.04 (q, 2H,CH_3CH_2O, J=4Hz), 4.19-4.26 (m, 1H, CHAla), 4.42 (bd, 2H,

CH_2benzylamine), 6.70 (bt, 1H, NH benzylamine), 7.01-8.49 (m, 13H, Ar), 10.16 (s, 1H, amide), 12.45 (bs, 1H, benzimidazole); MS: m/z (ESI) calcd for $[C_{35}H_{33}BrFN_5O_5]^+$: 701.16, found: 701.87.

Methyl 2-(2-(2-(4-((4-(3-bromo-4-methoxybenzamido)benzyl)amino)-3-fluorophenyl)-1*H*-benzo[*d*]imidazol-5-yl)acetamido)-3-phenylpropanoate (11c). Compound **11c** was prepared from **9a** by means of GP-B. Phenylalanine methyl ester hydrochloride (0.13 g, 0.60 mmol); *dry* THF/*dry* DMF (50 mL:3 mL); R_f (AcOEt/MeOH 4:1): 0.56; 83% as a white-yellow solid; 154-156°C; ethyl acetate; IR *v* 3273 (NH), 1738 (C=O), 1648, 1626 (C=O amide) cm^{-1}; ^1H NMR (DMSO d_6) δ 2.90-2.95 (m, 1H, CH_2PhAla), 3.00-3.05 (m, 1H, CH_2PhAla), 3.49-3.50 (m, 2H, CH_2acetic), 3.58 (s, 2H, CH_3O ester), 3.94 (s, 3H, OCH_3), 4.41-4.49 (m, 3H, CH_2benzylamine and CH PhAla), 6.71 (bt, 1H, NH benzylamine) 6.90-8.51 (m, 18H, Ar), 10.17 (s, 1H, amide), 12.47 (bs, 1H, benzimidazole); MS: m/z (ESI) calcd for $[C_{40}H_{35}BrFN_5O_5]^+$: 763.18, found: 764.

Ethyl (2-(2-(4-((4-(3-bromo-4-methoxybenzamido)benzyl)amino)-3-fluorophenyl)benzo[d]oxazol-5-yl)acetyl)glycinate (12a). Compound **12a** was prepared from **10a** by means of GP-B. L-Glycine ethyl ester hydrochloride (0.06 g, 0.40 mmol); 50 mL; R_f (ethyl acetate): 0.63; 88% as an yellow solid; 200-201°C; ethyl acetate; IR: *v* 3054 (NH), 1728 (C=O ester), 1649 (C=O amide), 1598 (C=O amide) cm^{-1}; ^1H NMR (DMSO d_6) δ 1.17 (t, 3H, $CH_2\underline{CH_3}$, J = 8 Hz), 3.60 (s, 2H, Ar$\underline{CH_2}$CO), 3.84 (d, 2H, NH$\underline{CH_2}$CO, J = 4 Hz), 3.93 (s, 3H, OCH_3), 4.08 (q, 2H, $\underline{CH_2}CH_3$, J = 8 Hz), 4.44 (br d, 2H, NH$\underline{CH_2}$), 6.76 (t, 1H, benzene H, J = 8 Hz), 7.11 (br t, 1H, $\underline{NH}CH_2$), 7.24 (t, 2H, benzoxazole C6-H and C4-H, J = 8 Hz), 7.36 (d, 2H, benzene H, J = 8 Hz), 7.59 (s, 1H, benzene H), 7.62 (d, 1H, benzoxazole C7-H, J = 8 Hz), 7.70-7.80 (m, 4H, benzene H), 8.00 (d, 1H, benzene H, J = 8 Hz), 8.22 (s, 1H, benzene H), 8.51 (t, 1H,

NHCH$_2$CO, J = 4 Hz), 10.18 (s, 1H, NHCO); MS: m/z (ESI) calcd for [$C_{34}H_{30}BrFN_4O_6$]$^-$: 688.13, found: 686.25.

Ethyl (2-(2-(4-((4-(3-bromo-4-methoxybenzamido)benzyl)amino)-3-fluorophenyl)benzo[d]oxazol-5-yl)acetyl)alaninate (12b). Compound **12b** was prepared from **10a** by means of GP-B. L-Alanine ethyl ester hydrochloride (0.09 g, 0.60 mmol); 50 mL; R_f (EtOAc/ MeOH 9:1): 0.66; 82% as a yellow solid; 235-238°C; ethyl acetate; IR *v* 3273 (NH), 1735 (C=O ester), 1673(C=O amide), 1628 (C=O amide) cm^{-1}; ^{1}H NMR (DMSO d_6) δ 1.14 (t, 3H, CH$_2$CH$_3$, J = 8 Hz), 1.29 (br d, 3H, CH$_3$CH), 3.57 (s, 2H, ArCH$_2$CO), 3.93 (s, 3H, OCH$_3$), 4.05 (q, 2H, CH$_2$CH$_3$, J = 8 Hz), 4.23 (m, 1H, CH$_3$CH), 4.44 (br d, 2H, NHCH$_2$Ph), 6.76 (t, 1H, benzene H, J = 8 Hz), 7.11 (br t, 1H, NHCH$_2$), 7.24 (t, 2H, benzoxazole C6-H and C4-H, J = 8 Hz), 7.36 (d, 2H, benzene H, J = 8 Hz), 7.57 (s, 1H, benzene H), 7.61 (d, 1H, benzoxazole C7-H,, J = 8 Hz), 7.70-7.80 (m, 4H, benzene H), 8.00 (d, 1H, benzene H, J = 8 Hz), 8.22 (s, 1H, benzene H), 8.51 (br d, 1H, NHCHCH$_3$), 10.18 (s, 1H, NHCO); MS: m/z (ESI) calcd for [$C_{35}H_{32}BrFN_4O_6$]$^-$: 702.15, found: 701.

Methyl (2-(2-(4-((4-(3-bromo-4-methoxybenzamido)benzyl)amino)-3-fluorophenyl)benzo[d]oxazol-5-yl)acetyl)phenylalaninate (12c). Compound **12c** was prepared from **10a** by means of GP-B. L-Phenylalanine methyl ester hydrochloride (0.13 g, 0.6 mmol); 50 mL; R_f (EtOAc/ MeOH 9:1): 0.87; 94% as a yellow solid; 162-164°C; washed with diethyl ether; IR *v* 3280 (NH), 1738 (C=O ester), 1644(C=O amide), 1623 (C=O amide) cm^{-1}; ^{1}H NMR (DMSO d_6) δ 2.99 (br d, 2H, CH$_2$CH), 3.53 (s, 2H, ArCH$_2$CO), 3.60 (s, 3H, COOCH$_3$), 3.93 (s, 3H, OCH$_3$), 4.44-4.50 (m, 1H, CH$_2$CH), 6.76 (t, 1H, benzene H, J = 8 Hz), 7.05-30 (m, 9H, NHCH$_2$ and PhCH$_2$), 7.36 (d, 1H, benzoxazole C6-H, J = 8 Hz), 7.49 (s, 1H, benzoxazole C4-H), 7.56 (s, 1H, benzoxazole C7-H, J = 8 Hz), 7.70-7.80 (m, 4H, benzene H), 8.00 (d, 1H, benzene

H, J = 8 Hz), 8.22 (s, 1H, benzene H), 8.41 (br d, 1H, COCHNH), 10.18 (s, 1H, NHCO); MS: m/z (ESI) calcd for $[C_{40}H_{34}BrFN_4O_6]^-$: 764.16, found: 763.

Dimethyl (2-(2-(4-((4-(3-bromo-4-methoxybenzamido)benzyl)amino)-3-fluorophenyl)benzo[d]oxazol-5-yl)acetyl)glutamate (12d). Compound **12d** was prepared from **10a** by means of GP-B. L-Glutamic acid dimethyl ester hydrochloride (0.13 g, 0.60 mmol); 50 mL; R_f (EtOAc/ MeOH 9:1): 0.87; 70% as a yellow-green solid; 182-184°C; ethyl acetate; IR *v* 3265 (NH), 1732 (C=O ester), 1673 (C=O amide), 1647 (C=O amide) cm^{-1}; ^1H NMR (DMSO d_6) δ 1.75-1.80 (m, 1H, αCH$_2$), 1.90-2.00 (m, 1H, αCH$_2$), 2.27 (t, 2H, βCH$_2$, J = 8 Hz), 3.55-3.65 (m, 8H, ArCH$_2$CO and COOCH$_3$), 3.93 (s, 3H, OCH$_3$), 4.24-4.32 (m, 1H, CH$_3$OCOCH), 4.44 (br d, 2H, PhCH$_2$NH), 6.76 (t, 1H, benzene H, J = 8 Hz), 7.11 (br t, 1H, NHCH$_2$), 7.25 (t, 2H, benzoxazole C6-H and benzoxazole C4-H, J = 8 Hz), 7.36 (s, 1H, benzene H, J = 8 Hz), 7.56-7.61 (m, 3H, benzoxazole C7-H and benzene H), 7.70-7.80 (m, 4H, benzene H), 8.00 (d, 1H, benzene H, J = 8 Hz), 8.22 (s, 1H, benzene H), 8.39 (br d, 1H, CONHCH), 10.17 (s, 1H, Ar-NHCO); MS: m/z (ESI) calcd for $[C_{37}H_{34}BrFN_4O_8]^-$: 760.15, found: 759.

Methyl N^6-(((9H-fluoren-9-yl)methoxy)carbonyl)-N^2-(2-(2-(4-((4-(3-bromo-4-methoxybenzamido)benzyl)amino)-3-fluorophenyl)benzo[d]oxazol-5-yl)acetyl)lysinate (12e). Compound **12e** was prepared from **10a** by means of GP-B. $N^ε$-Fmoc-L-lysine methyl ester hydrochloride (0.42 g, 1 mmol), 50 mL; R_f (EtOAc/ MeOH 9:1): 0.87; 80% as a yellow solid; 172-174°C; washed with dichloromethane; IR *v* 3293 (NH), 1724 (C=O ester), 1646 (C=O amide), 1622 (C=O amide), 1599 (C=O amide) cm^{-1}; ^1H NMR (DMSO d_6) δ 1.18-1.37 (m, 6H, γ-εCH$_2$ -Lys), 2.93-2.95 (d, H, CH- Fmoc, J=8 Hz), 3.58-3.64 (m, 5H NHCOCH$_2$-Ar and COOCH$_3$), 3.94 (s, 3H, OCH$_3$), 4.16 (br m, 1H, αCH-Lys), 4.29 (d, 2H, O-CH$_2$-fluorene, J=8 Hz), 4.44 (d, 2H, CH$_2$ benzylamine, J=8 Hz), 6.06 (br s, 1H, NH-Fmoc), 6.75-6.77 (br t, 1H,

benzene H), 7.11 (br t, 1H NH benzylamine), 7.21-7.74 (m, 18 H, fluorene H, benzoxazole C6-H, benzoxazole C4-H and benzene H), 7.92 (d, 1H, benzoxazole C7-H, J = 8 Hz), 8.21 (d, 2H, benzene H J=4), 8.52 (br s, 1H, Ar-NHCO-Ar); MS: m/z (ESI) calcd for $[C_{52}H_{47}BrFN_5O_8]^-$: 967.26, found: 966.

2-(2-(2-(4-((4-(3-bromo-4-methoxybenzamido)benzyl)amino)-3-fluorophenyl)-1*H*-benzo[*d*]imidazol-5-yl)acetamido)acetic acid (13a). Compound **13a** was prepared from **11a** by means of GP-A. **11a** (0.15 g, 0.22mmol); 21 mL; 0.18 (AcOEt/MeOH 3:2); 100% as an orange solid; 187-189 °C; isopropanol; IR *v* 3314 (NH benzylamine), 2842 (OH), 1731 (C=O acid), 1618, 1600 (C=O amide) cm^{-1}; ^1H NMR (DMSO d_6) δ 3.64 (s, 2H, CH_2 acetic), 3.76 (bd, 2H, CH_2Gly), 3.93(s, 3H, OCH_3), 4.46 (bd, 2H, CH_2benzylamine), 6.84 (bt, 1H, NH benzylamine), 7.23-8.42 (m, 13H, Ar), 10.18 (s, 1H, amide), 12.55 (bs, 1H, benzimidazole), 14.31 (bs, 1H, OH); MS: m/z (ESI) calcd for $[C_{32}H_{27}BrFN_5O_5]^+$: 659.12, found: 660.07.

2-(2-(2-(4-((4-(3-bromo-4-methoxybenzamido)benzyl)amino)-3-fluorophenyl)-1*H*-benzo[*d*]imidazol-5-yl)acetamido)propanoic acid (13b). Compound **13b** was prepared from **11b** by means of GP-A. **11b** (0.29 g, 0.41 mmol); 10 mL; R_f (AcOEt/MeOH 3:2): 0.23; 98% as an orange solid; 175-178°C; isopropanol; IR *v* 3280 (NH benzylamine), 2939 (OH), 1724 (C=O acid), 1619 (C=O amide) cm^{-1}; ^1H NMR (DMSO d_6) δ 1.27 (d, 3H, CH_3Ala, J=4 Hz), 3.62 (s, 2H, CH_2 acetic), 3.93 (s, 3H, OCH_3), 4.17-4.23 (m, 1H, CH Ala), 4.47 (bd, 2H, CH_2benzylamine), 6.84 (t, 1H, NH benzylamine, J=8 Hz), 7.23-8.49 (m, 13H, Ar), 10.19 (s, 1H, amide), 12.52 (bs, 1H, benzimidazole), 14.55 (br s, 1H, OH); MS: m/z (ESI) calcd for $[C_{33}H_{29}BrFN_5O_5]^+$: 673.13, found: 674.

2-(2-(2-(4-((4-(3-bromo-4-methoxybenzamido)benzyl)amino)-3-fluorophenyl)-1*H*-benzo[*d*]imidazol-5-yl)acetamido)-3-phenylpropanoic acid (13c). Compound **13c** was

prepared from **11c** by means of GP-A. **11c** (0.3 g, 0.39 mmol); 10 mL; R_f (AcOEt:MeOH 3:2): 0.29; 92% as a yellow solid; 179-181°C; isopropanol; IR *v* 3300 (NH benzylamine), 2938 (OH), 1731 (C=O acid), 1620, 1600 (C=O amide) cm^{-1}; ^1H NMR (DMSO d_6) δ 2.84-2.90 (m, 1H, CH_2PhAla), 3.02-3.06 (m, 1H, CH_2PhAla), 3.51-3.52 (m, 2H, CH_2 acetic), 3.93 (s, 3H, OCH_3), 4.38-4.43 (m, 3H, CH PhAla and CH_2benzylamine), 6.75 (t, 1H, NH benzylamine, J=8 Hz), 6.87-8.35 (m, 13H, Ar), 10.16 (s, 1H, amide), 12.72 (bs, 1H, benzimidazole), 14.31 (bs, 1H, OH); MS: m/z (ESI) calcd for $[C_{39}H_{33}BrFN_5O_5]^+$: 749.16, found: 750.00.

((2-(2-(4-((4-(3-bromo-4-methoxybenzamido)benzyl)amino)-3-fluorophenyl)-1H-benzo[d]imidazol-5-yl)acetamido)methyl)boronic acid (13d). Compound **13d** was prepared from **9a** by means of GP-C. **27a** (0.10 g, 0.13 mmol); THF 5 mL; R_f (EtOAc:MeOH 9:1): 0.43; 35% as an orange solid; 241-242°C; washed with diethyl ether; IR *v* 3278 (OH), 2944 (NH), 1621 (C=O amide), 1599 (C=O amide) cm^{-1}. ^1H NMR (DMSO d_6) δ 3.49 (s, 2H, Ar$\underline{CH_2}$CO), 3.93 (s, 3H, OCH_3), 4.42 (br d, 2H, Ar$\underline{CH_2}$NH), 4.50 (br d, 2H, CH_2B), 6.71-6.76 (m, 1H, benzene H, and Ar-$NHCH_2$), 7.05-7.07 (m, 2H, benzimidazole C6-H and C4-H), 7.24-7.26 (d, 2H, benzene H, J = 8 Hz), 7.35-7.44 (m, 4H, benzene H and benzimidazole C7-H), 7.76-7.83 (m, 3H, benzene H), 8.05 (d, 1H, benzene H, J = 8 Hz), 8.22 (s, 1H, benzene H), 8.60 (br t, 1H, $CH_2\underline{NH}$CO), 8.83 (br s, 2H, OH), 10.17 (s, 1H, NHCO); 98.43%; MS: m/z (ESI) calcd for $[C_{31}H_{28}BBrFN_5O_5]^-$: 659.14, found: 631.80 (M^--BOH).

(2-(2-(4-((4-(3-bromo-4-methoxybenzamido)benzyl)amino)-3-fluorophenyl)benzo[d]oxazol-5-yl)acetyl)glycine (14a). Compound **14a** was prepared from **12a** by means of GP-A. **12a** (0.15 g, 0.22 mmol), 20 mL; R_f (EtOAc: MeOH 7:3): 0.23; 70% as a yellow solid; washed with THF; IR: *v* 3424 (OH), 3054 (NH), 1726 (C=O acid), 1650, 1597 (C=O amide) cm^{-1}; ^1H NMR (DMSO d_6) δ 3.60 (s, 2H, Ar$\underline{CH_2}$CO), 3.84 (d, 2H, NH$\underline{CH_2}$CO, J =

4 Hz), 3.93 (s, 3H, OCH_3), 4.44 (br d, 2H, $NHCH_2Ph$), 6.76 (t, 1H, benzene H, J = 8 Hz), 7.11 (br t, 1H, $NHCH_2$), 7.24 (t, 2H, benzoxazole C6-H and C4-H, J = 8 Hz), 7.36 (d, 2H, benzene H, J = 8 Hz), 7.59 (s, 1H, benzene H), 7.62 (d, 1H, benzoxazole C7-H,, J = 8 Hz), 7.70-7.80 (m, 4H, benzene H), 8.00 (d, 1H, benzene H, J = 8 Hz), 8.22 (s, 1H, benzene H), 8.51 (t, 1H, $NHCH_2CO$, J = 4 Hz), 10.18 (s, 1H, NHCO); MS: m/z (ESI) calcd for $[C_{32}H_{26}BrFN_4O_6]^-$: 660.10, found: 658.90.

(2-(2-(4-((4-(3-bromo-4-methoxybenzamido)benzyl)amino)-3-fluorophenyl)benzo[d]oxazol-5-yl)acetyl)alanine (14b). Compound **14b** was prepared from **12b** by means of GP-A. **12b** (0.15 g, 0.21 mmol); 20 mL; R_f (EtOAc/ MeOH 7:3): 0.18; 70% as a yellow-orange solid; 200°C; washed with THF; IR *v* 3438 (OH), 3304 (NH), 1732 (C=O acid), 1630 (C=O amide), 1599 (C=O amide) cm^{-1}**;** ^{1}H NMR (DMSO d_6) δ 1.29 (br d, 3H, CH_3CH), 3.57 (s, 2H, $ArCH_2CO$), 3.93 (s, 3H, OCH_3), 4.23 (m, 1H, CH_3CH), 4.44 (br d, 2H, $NHCH_2Ph$), 6.76 (t, 1H, benzene H, J = 8 Hz), 7.11 (br t, 1H, $NHCH_2$), 7.24 (t, 2H, benzoxazole C6-H and C4-H, J = 8 Hz), 7.36 (d, 2H, benzene H, J = 8 Hz), 7.57 (s, 1H, benzene H), 7.61 (d, 1H, benzoxazole C7-H, J = 8 Hz), 7.70-7.80 (m, 4H, benzene H), 8.00 (d, 1H, benzene H, J = 8 Hz), 8.22 (s, 1H, benzene H), 8.51 (br d, 1H, $NHCHCH_3$), 10.18 (s, 1H, NHCO), 12.49 (s, 1H, COOH); MS: m/z (ESI) calcd for $[C_{33}H_{28}BrFN_4O_6]^-$: 674.12, found: 672.47.

(2-(2-(4-((4-(3-bromo-4-methoxybenzamido)benzyl)amino)-3-fluorophenyl)benzo[d]oxazol-5-yl)acetyl)phenylalanine (14c). Compound **14c** was prepared from **12c** by means of GP-A. **12c** (0.15 g, 0.19 mmol); 20 mL; R_f (EtOAc/ MeOH 7:3): 0.17; 60% as an orange solid; 152°C; washed with THF; IR *v* 3285 (OH), 2924 (NH) 1723 (C=O acid), 1649 (C=O amide), 1623 (C=O amide) cm^{-1}; ^{1}H NMR (DMSO d_6) δ 2.99 (br d, 2H, CH_2CH), 3.53 (s, 2H, $ArCH_2CO$), 3.60 (s, 3H, $COOCH_3$), 4.44-4.50 (m, 1H, CH_2CH), 6.76 (t, 1H, benzene

H, J = 8 Hz), 7.05-30 (m, 9H, NHCH$_2$ and PhCH$_2$), 7.36 (d, 1H, benzoxazole C6-H, J = 8 Hz), 7.49 (s, 1H, benzoxazole C4-H), 7.56 (s, 1H, benzoxazole C7-H, J = 8 Hz), 7.70-7.80 (m, 4H, benzene H), 8.00 (d, 1H, benzene H, J = 8 Hz), 8.22 (s, 1H, benzene H), 8.41 (br d, 1H, COCHNH), 10.18 (s, 1H, NHCO), 12.60 (s, 1H, COOH); MS: m/z (ESI) calcd for $[C_{39}H_{32}BrFN_4O_6]^-$: 750.15, found: 750.47.

(2-(2-(4-((4-(3-bromo-4-methoxybenzamido)benzyl)amino)-3-fluorophenyl)benzo[d]oxazol-5-yl)acetyl)glutamic acid (14d). Compound **14d** was prepared from **12d** by means of GP-A. **12d** (0.15 g, 0.19 mmol); 20 mL; R_f (EtOAc/ MeOH 7:3): 0.63; 72% as an orange solid; 197-199°C; washed with THF; IR *ν* 3313 (OH), 2944 (NH) 1716 (C=O acid), 1621 (C=O amide), 1598 (C=O amide) cm^{-1}; ^{1}H NMR (DMSO d_6) δ 1.75-1.80 (m, 1H, αCH$_2$), 1.90-2.00 (m, 1H, αCH$_2$), 2.27 (t, 2H, βCH$_2$, J = 8 Hz), 3.55-3.65 (s, 2H, ArCH$_2$CO), 3.93 (s, 3H, OCH$_3$), 4.24-4.32 (m, 1H, CH$_3$OCOCH), 4.44 (br d, 2H, PhCH$_2$NH), 6.76 (t, 1H, benzene H, J = 8 Hz), 7.11 (br t, 1H, NHCH$_2$), 7.25 (t, 2H, benzoxazole C6-H and benzoxazole C4-H, J = 8 Hz), 7.36 (s, 1H, benzene H, J = 8 Hz), 7.56-7.61 (m, 3H, benzoxazole C7-H and benzene H), 7.70-7.80 (m, 4H, benzene H), 8.00 (d, 1H, benzene H, J = 8 Hz), 8.22 (s, 1H, benzene H), 8.39 (br d, 1H, COCHNH), 10.17 (s, 1H, NHCO), 12.50 (s, 2H, COOH); MS: m/z (ESI) calcd for $[C_{35}H_{30}BrFN_4O_8]^-$: 732.12, found: 732.67.

(2-(2-(4-((4-(3-bromo-4-methoxybenzamido)benzyl)amino)-3-fluorophenyl)benzo[*d*]oxazol-5-yl)acetyl)lysine (14e). Compound **14e** was prepared from **12e** by means of GP-A. **14e** (0.02 mg, 0.027 mmol); 5 mL; R_f (ethyl acetate/methanol 1:1): 0.3; 51% as a grey solid; 214-216 °C; washed with THF; IR ν 3439 (various NH), 2940 (OH), 1728 (C=O), 1625 (C=O) cm-1; ^{1}H NMR (DMSO d_6) δ 1.15-1.72 (m, 6H, γ-εCH$_2$-Lys), 3.58 (s, 2H, NHCOCH$_2$-Ar), 3.58 (s, 2H, βCH$_2$-Lys), 3.93 (s, 3H, OCH$_3$), 4.16 (br m, 1H, αCH-Lys), 4.43

(br d, 2H, CH_2 benzylamine), 6,76-8.21 (m, 14H, benzoxazole C6-H, benzoxazole C4-H and benzene H and NH benzylamine), 8.37 (br d, 1H, Ar-NHCO-Ar), 10.17 (s, 1H, Ar-NHCO-Ar), 12.5 (br s, 1H, OH); MS: m/z (ESI) calcd for $[C_{36}H_{35}BrFN_5O_6]^+$: 731.18, found: 732.00.

((2-(2-(4-((4-(3-bromo-4-methoxybenzamido)benzyl)amino)-3-fluorophenyl)benzo[d]oxazol-5-yl)acetamido)methyl)boronic acid (14f). Compound **14f** was prepared from **10a** by means of GP-C. **10a** (0.15 g, 0.20 mmol); acetone 5.2 mL; R_f (EtOAc): 0.4; 38% as a yellow solid; 191-193°C; washed with diethyl ether; IR *v* 3429 (OH), 3297 (NH), 1651 (C=O amide), 1621 (C=O amide)cm^{-1}. ^1H NMR (DMSO d_6) δ 2.20 (br d, 1H, CH_2B), 3.57 (s, 2H, Ar$\underline{CH_2}$CO), 3.74 (br d, 1H, CH_2B), 3.98 (s, 3H, OCH_3), 4.49 (br d, 2H, Ar$\underline{CH_2}$NH), 6.81 (t, 1H, benzene H, J = 8 Hz), 7.15 (br t, 1H, $\underline{NH}CH_2$), 7.28-7.31 (m, 2H, benzoxazole C6-H and C4-H), 7.40 (d, 2H, benzene H, J = 8 Hz), 7.57-7.62 (m, 2H, benzene H and benzoxazole C7-H), 7.76-7.83 (m, 3H, benzene H), 8.05 (d, 1H, benzene H, J = 8 Hz), 8.27 (s, 1H, benzene H), 8.72 (br t, 1H, $CH_2\underline{NH}CO$), 8.83 (br s, 2H, OH), 10.22 (s, 1H, NHCO); MS: m/z (ESI) calcd for $[C_{31}H_{27}BBrFN_4O_6]^-$: 660.12, found: 660.40.

Synthesis of 2-(4-(4-(3-bromo-4-methoxybenzamido)benzyl)amino)-3-fluorophenyl)-1*H*benzo[*d*]imidazole (15). Compound **26** (70 mg, 0.13 mmol) was dissolved in *N*,*N*-dimethylformamide and sodium borohydride (8 mg, 0.21 mmol) was added under stirring at room temperature. After 2 hours starting material was totally converted. The mixture pH was neutralized to 7 by HCl 3N addition; after concentration under reduced pressure, the crude product was purified by silica gel chromatography (eluent dichloromethane/methanol 97:3) to give about 50 mg of compound **15** as a pure light yellow solid. Yield 70%. ^1H NMR (DMSO d_6) δ 3.94 (s, 3H), 4.45 (s, 2H), 6.81 (t, *J* = 7.0 Hz, 1H), 7.08 (bs, 1H), 7.25 (d, *J* = 7.8 Hz, 1H), 7.30 (bs, 2H), 7.37 (d, *J* = 6.8 Hz, 2H), 7.93 (bs, 2H), 7.72 (d, *J* = 6.8 Hz, 2H), 7.80 (d, *J* = 7.3 Hz,

1H), 7.93 (d, *J* = 12.2 Hz, 1H), 8.01 (d, *J* = 7.8 Hz, 1H), 8.22 (s, 1H), 10.19 (s,1H). MS: m/z (ESI) calcd for $[C_{28}H_{22}BrFN_4O_2]^+$: 544.09, found: 545 and 567 ($M+Na^+$); MS: m/z (ESI) calcd for $[C_{28}H_{22}BrFN_4O_2]^-$: 544.09, found: 543.

Methyl 2-(3,4-diaminophenyl)acetate (16). Compound **16** was prepared according to literature.[23] Analytical data are herein reported.

Methyl 2-(2-(3-fluoro-4-nitrophenyl)-1*H*-benzo[*d*]imidazol-5-yl)acetate (17a). Compound **17a** was prepared from **16** by means of GP-D. 3-fluoro-4-nitrobenzaldehyde (25 g, 150 mmol); Rf (*n*-hexane/Et_2O 1:9):0.37; 65% as a yellow solid; 169-172°C; IR *v* 3068 (NH), 1716 (C=O ester) cm^{-1}; ^1H NMR (DMSO d_6) δ 3.63 (s, 3H, OCH_3), 3.83 (s, 2H, CH_2acetic), 7.18-8.40 (m, 6H, Ar), 13.31 (br s, 1H, benzimidazole); MS: m/z (ESI) calcd for $[C_{16}H_{12}FN_3O_4]^+$: 329.08, found: 330.

Methyl 2-(2-(4-nitrophenyl)-1*H*-benzo[*d*]imidazol-5-yl)acetate (17b). Compound **17b** was prepared from **16** by means of GP-D. 4-nitrobenzaldehyde (2.68 g, 18 mmol); R_f (n-hexane/Et_2O 9:1): 0.36; 69% as a yellow solid; 131-134°C; IR *v* 3049 (NH), 1716 (C=O ester) cm^{-1}; ^1H NMR (DMSO d_6) δ 3.62 (s, 3H, OCH_3), 3.82 (s, 2H, CH_2 acetic), 7.16-8.41 (m, 7H, Ar), 13.26 (br s, 1H, benzimidazole); MS: m/z (ESI) calcd for $[C_{16}H_{13}N_3O_4]^+$: 311.09, found: 312.

Methyl 2-(2-(4-amino-3-fluorophenyl)-1*H*-benzo[*d*]imidazol-5-yl)acetate (18a). Compound **18a** was prepared from **17a** by means of GP-E. **17a** (0.79 g, 2.4 mmol); AcOEt 158 mL; R_f (*n*-hexane/AcOEt 1:1): 0.15; 100% as a white solid; 247-250°C; IR *v* 3347 (NH), 3147 (NH_2), 1720 (C=O ester) cm^{-1}; ^1H NMR (DMSO d_6) δ 3.61 (s, 3H, OCH_3), 3.73-3.76 (m, 2H, CH_2 acetic), 5.67 (s, 2H, NH_2), 6.83-7.76 (m, 6H, Ar), 12.51 (bs, 1H, benzimidazole); MS: m/z (ESI) calcd for $[C_{16}H_{14}FN_3O_2]^+$: 299.31, found: 300.

Methyl 2-(2-(4-aminophenyl)-1*H*-benzo[*d*]imidazol-5-yl)acetate (18b). Compound **18b** was prepared from **17b** by means of GP-E. **17b** (1.5 g, 4.8 mmol); MeOH 50mL; R_f (AcOEt): 0.24; 70% as a pink solid; 213-215°C; IR *v* 3216 (NH), 3141 (NH_2), 1716 (C=O ester) cm^{-1}; ^1H NMR (DMSO d_6) δ 3.61 (s, 3H, OCH_3), 3.73-3.75 (m, 2H, CH_2 acetic), 5.59 (s, 2H, NH_2), 6.64-7.82 (m, 7H, Ar), 12.37 (bs, 1H, benzimidazole); MS: m/z (ESI) calcd for $[C_{16}H_{15}N_3O_2]^+$: 281.32, found: 282.

Methyl 2-(2-(4-amino-3-fluorophenyl)benzo[d]oxazol-5-yl)acetate (19a). Compound **19a** was prepared according to literature.[22] Analytical data are herein reported.

Methyl 2-(2-(4-aminophenyl)benzo[d]oxazol-5-yl)acetate (19b). Compound **19b** was prepared according to literature.[22] Analytical data are herein reported.

Methyl 2-(2-(4-((4-(3-bromo-4-methoxybenzamido)benzylidene)amino)-3-fluorophenyl)-1*H*-benzo[*d*]imidazol-5-yl)acetate (20a). Compound **20a** was prepared from **18a** by means of GP-F. **18a** (0.74 g, 2.5 mmol); R_f ($CHCl_3$/MeOH 8.5:1.5): 0.78; 72% as a yellow solid; 230-232°C; IR *v* 3329 (NH), 1716 (C=O ester), 1655 (C=O amide), 1634 (C=N) cm^{-1}; ^1H NMR (DMSO d_6) δ 3.63 (s, 3H, $COOCH_3$), 3.78-3.81 (m, 2H, CH_2 acetic), 3.95 (s, 3H, OCH_3), 7.09-8.28 (m, 13H, Ar), 8.71 (s, 1H, H imine), 10.49 (s, 1H, amide), 12.92 (bs, 1H, benzimidazole); MS: m/z (ESI) calcd for $[C_{31}H_{24}BrFN_4O_4]^+$: 614.10, found: 615.

Methyl 2-(2-(4-((4-(3-bromo-4-methoxybenzamido)benzylidene)amino)phenyl)-1*H*-benzo[*d*]imidazol-5-yl)acetate (20b). Compound **20b** was prepared from **18b** by means of GP-F. **18b** (0.93 g, 3.31 mmol); R_f ($CHCl_3$/MeOH 8.5:1.5): 0.68; 82% as a yellow solid; 221-224°C; IR *v* 3267 (NH), 1736 (C=O ester), 1661 (C=O amide), 1627 (C=N) cm^{-1}; ^1H NMR (DMSO d_6) δ 3.63 (s, 3H, $COOCH_3$), 3.79 (s, 2H, CH_2 acetic), 3.95 (s, 3H, OCH_3), 7.09-8.27 (m, 14H, Ar),

8.67 (s, 1H, H imine), 10.46 (s, 1H, amide), 12.88 (bs, 1H, benzimidazole); MS: m/z (ESI) calcd for $[C_{31}H_{25}BrN_4O_4]^+$: 596.11, found: 597.

Methyl (E)-2-(2-(4-((4-(3-bromo-4-methoxybenzamido)benzylidene)amino)-3-fluorophenyl)benzo[d]oxazol-5-yl)acetate (21a). Compound **21a** was prepared from **19a** by means of GP-F. **19a** (0.3 g, 1 mmol); R_f (*n*-hexane/ethyl acetate 1:1): 0.6; 77% as a yellow solid; 238 °C; IR ν 1731 (C=O ester), 1635 (N=CH immine) cm^{-1}; ^1H NMR (DMSO d_6) δ 3.65 (s, 3H, CH_3,), 3.86 (s, 2H, CH_2), 3.96 (s, 3H, OCH_3), 7.29 (d, 1H, benzene H, J = 8 Hz), 7.36 (d, 1H, benzene H, J= 8 Hz), 7.55 (t, 1H, benzene H, J = 8 Hz), 7.73-7.77 (m, 2 H, benzoxazole C4-H and C6-H), 8.00-8.10 (m, 6H, benzene H and benzoxazole C7-H,), 8.28 (br d, 1H, benzene H), 8.71 (s, 1H, NCH), 10.51 (s, 1H, NHCO); MS: m/z (ESI) calcd for $[C_{31}H_{23}BrFN_3O_5]^+$: 615.08, found: 616.

Methyl (E)-2-(2-(4-((4-(3-bromo-4-methoxybenzamido)benzylidene)amino)phenyl)benzo[d]oxazol-5-yl)acetate (21b). Compound **21b** was prepared from **19b** by means of GP-F. **19b** (0.7 g, 2.48 mmol); R_f (*n*-hexane/ethyl acetate 1:1): 0.4; 70% as a yellow solid; 235 °C; IR ν 1731 (C=O ester), 1635 (N=CH immine) cm^{-1}; ^1H NMR (DMSO d_6) δ 3.65 (s, 3H, CH_3), 3.85 (s, 2H, CH_2), 3.96 (s, 3H, OCH_3), 7.25-7.35 (m, 2H, benzene H and benzoxazole C6-H), 7.47 (d, 2H, benzene H, J = 8 Hz), 7.70-7.75 (m, 2 H, benzoxazole C4-H and benzene H), 8.00-8.10 (m, 5H, benzene H), 8.23-8.27 (m, 3H, benzene H), 8.66 (s, 1H, N=CH), 10.47 (s, 1H, NHCO); MS: m/z (ESI) calcd for $[C_{31}H_{24}BrN_3O_5]^+$: 597.09, found: 598.

Methyl 2-(2-(4-((4-(3-bromo-4-methoxybenzamido)benzyl)amino)-3-fluorophenyl)-1*H*-benzo[*d*]imidazol-5-yl)acetate (22a). Compound **22a** was prepared from **20a** by means of GP-G.

20a (1.06 g, 1.7 mmol); 50 mL; 0.2 g (5.3 mmol) within 23 h; R_f (AcOEt): 0.7; 100% as a white solid; 200-202°C; washed with diethyl ether; IR *v* 3254 (NH), 1722 (C=O ester), 1625 (C=O amide) cm^{-1};^{1}H NMR (DMSO d_6) δ 3.61 (s, 3H, $COOCH_3$), 3.74 (s, 2H, CH_2 acetic), 3.93 (s, 3H, OCH_3), 4.40 (bd, 2H, CH_2benzylamine), 6.71 (bt, 1H, NH benzylamine), 7.00-8.21 (m, 13H, Ar), 10.16 (s, 1H, amide), 12.52 (bs, 1H, benzimidazole); MS: m/z (ESI) calcd for $[C_{31}H_{26}BrFN_4O_4]^+$: 617.48, found: 618.

Methyl 2-(2-(4-((4-(3-bromo-4-methoxybenzamido)benzyl)amino)phenyl)-1*H*-benzo[*d*]imidazol-5-yl)acetate (22b). Compound **22b** was prepared from **20b** by means of GP-G. **20b** (0.15 g, 0.25 mmol); 7 mL; 0.1 g (2.64 mmol) within 15 h; R_f (AcOEt): 0.68; 100% as a white solid; 123-126°C; washed with diethyl ether; IR *v* 3329 (NH_2), 1720 (C=O ester), 1649 (C=O amide) cm^{-1}; ^{1}H NMR (DMSO d_6) δ 3.60 (s, 3H, $COOCH_3$), 3.72-3.75 (m, 2H, CH_2 acetic), 3.93 (s, 3H, OCH_3), 4.33 (bd, 2H, CH_2benzylamine), 6.62 (bt, 1H, NH benzylamine), 6.69-8.22 (m, 14H, Ar), 10.17 (s, 1H, amide), 12.38 (bs, 1H, benzimidazole); MS: m/z (ESI) calcd for $[C_{31}H_{27}BrN_4O_4]^+$: 598.12, found: 599.

Methyl 2-(2-(4-((4-(3-bromo-4-methoxybenzamido)benzyl)amino)-3-fluorophenyl)benzo[d]oxazol-5-yl)acetate (23a). Compound **23a** was prepared from **21a** by means of GP-G. **21a** (0.48 g, 0.77 mmol); 20 mL; 0.4 g (10.56 mmol) within 15 h; R_f (*n*-hexane/ethyl acetate 1:1): 0.5; 100% as a yellow solid; 238 °C; washed with diethyl ether; IR ν 3375 (NH) 1732 (C=O ester), 1650 (C=O amine) cm^{-1}; ^{1}H NMR (DMSO d_6) δ 3.63 (s, 3H, $COOCH_3$), 3.81 (s, 2H, $OCOCH_2$), 3.93 (s, 3H, OCH_3), 4.44 (br d, 2H, $NH\underline{CH_2}$), 6.76 (t, 1H, benzene H, J = 8 Hz), 7.13 (br t, 1H, $\underline{NH}CH_2$), 7.24 (t, 2H, benzoxazole C6-H and C4-H, J = 8 Hz), 7.36 (d, 2H, benzene H, J = 8 Hz), 7.59 (s, 1H, benzoxazole C4-H), 7.63 (d, 1H, benzoxazole C7-H,, J = 8 Hz), 7.70-7.80 (m, 4H, benzene H), 8.00 (br d, 1H, benzene H), 8.22

(s, 1H, benzene H), 10.18 (s, 1H, NHCO); MS: m/z (ESI) calcd for $[C_{31}H_{25}BrFN_3O_5]^+$: 617.10, found: 618.

Methyl 2-(2-(4-((4-(3-bromo-4-methoxybenzamido)benzyl)amino)phenyl)benzo[d]oxazol-5-yl)acetate (23b). Compound **23b** was prepared from **21b** by means of GP-G. **21b** (0.5 g, 0.83 mmol); 40 mL; 0.4 g (10.56 mmol) within 15 h; R_f (*n*-hexane/ethyl acetate 1:1): 0.62; 60% as a yellow solid; 230-231 °C; washed with diethyl ether; IR ν 3374 (NH) 1733 (C=O ester), 1648 (C=O amine) cm^{-1}; ^1H NMR (DMSO d_6) δ 3.63 (s, 3H, $COOCH_3$), 3.79 (s, 2H, $OCOCH_2$), 3.94 (s, 3H, OCH_3), 4.36 (br d, 2H, $NHCH_2$), 6.75 (d, 2H, benzene H, J = 8 Hz), 7.13 (br t, 1H, $NHCH_2$), 7.20 (d, 1H, benzoxazole C6-H, J = 8 Hz), 7.25 (d, 1H, benzene H, J = 8 Hz), 7.35 (d, 2H, benzene H, J = 8 Hz), 7.55 (s, 1H, benzoxazole C4-H), 7.60 (d, 1H, benzoxazole C7-H, J = 8 Hz), 7.72 (d, 2H, benzene H, J = 8 Hz), 7.89 (d, 2H, benzene H, J = 8 Hz), 8.01 (d, 1H, benzene H, J = 8 Hz), 8.22 (s, 1H, benzene H), 10.18 (s, 1H, NHCO); 95.62%; MS: m/z (ESI) calcd for $[C_{31}H_{26}BrN_3O_5]^+$: 599.11, found: 600.

Synthesis of methyl (2-(2-(4-((4-(3-bromo-4-methoxybenzamido)benzyl)amino)-3-fluorophenyl)benzo[*d*]oxazol-5-yl)acetyl)lysinate (24). A round-bottom flask was charged with **12e** (100 mg, 0.10 mmol) and a solution of 20% (v/v) piperidine in dry DMF (freshly prepared) was added in one portion, and the mixture was stirred at room temperature for 30 min under argon atmosphere, following a known procedure.[25] Upon reaction completed, the mixture was poured into water and the solid that formed was filtered, washed with hexane and dried under IR lamp to afford the pure product as a white solid. R_f (ethyl acetate/chloroform 7:3): 0.19; 100%; 197 °C; IR *v* 3450 (NH_2), 2910 (NH), 1731 (C=O ester), 1623 (C=O amide), 1618 (C=O amide) cm^{-1}; ^1H NMR (DMSO d_6) δ 1.35-1.64 (m, 8H, γ-εCH_2 -Lys), 3.62 (s, 2H, $NHCOCH_2$-Ar), 3.59-3.65 (m, 5H $NHCOCH_2$-Ar and $COOCH_3$), 3.93 (s, 3H, OCH_3), 6,75-8.21 (m, 14H, benzoxazole

C6-H, benzoxazole C4-H and benzene H and NH benzylamine), 8.52 (br s, 1H, Ar-NHCO-Ar), 10.17 (br s, 1H, Ar-NHCO-Ar); 98.01%; MS: m/z (ESI) calcd for $[C_{37}H_{37}BrFN_5O_6]^+$: 746.63, found: 748.13.

Synthesis of 4-(1*H*-benzo[d]imidazol-2-yl)-2-fluoroaniline (25). 1,2-Phenylendiamine (6.5 g, 60 mmol), 3-fluoro-4-aminobenzoic acid (7.9 g, 51 mmol) and polyphosphoric acid (25 g) were put in a round flask and stirred a 220 °C for 5 hours (a dark oily mixture formed almost immediately). After cooling, potassium carbonate (10%, 400 mL) was added to this dark oily crude; the lump formed, was neutralized to pH=7 with saturated solution of $NaHCO_3$ and, after lump turned to suspension, the solid was recovered by filtration. The crude product was washed with hot water (50-70 °C) till the water was colorless and, after crystallization by ethyl acetate (1 L) and filtration on charcoal, compound **25** (7 g) was obtained as a pure light brown solid. Yield 60%. ^{1}H NMR (DMSO d_6) δ 5.66 (s, 2H), 6.86 (t, J = 8.8 Hz, 1H), 7.13 (m, 2H), 7.50 (bs, 2H), 7.72 (d, J = 8.3 Hz, 1H), 7.78 (dd, J_1=12.7 Hz, J_2 = 1.5 Hz, 1H), 12.56 (bs, 1H). MS: m/z (ESI) calcd for $[C_{13}H_{10}FN_3]^+$: 227.09, found 228; MS: m/z (ESI) calcd for $[C_{13}H_{10}FN_3]^-$: 226.

Synthesis of methyl 2-(2-(4-((4-(3-bromo-4-methoxybenzamido)benzyl)amino)-3-fluorophenyl)benzo[d]oxazol-5-yl)acetate (26). Compound **25** (50 mg, 0.22 mmol) and 3-bromo-*N*-(4-formylphenyl)-4-methoxybenzamide[20] (73 mg, 0.22 mmol) were suspended in ethanol (5 mL) with few drops of acetic acid and the mixture was warmed at 70 °C. After few minutes starting materials were completely dissolved and a new precipitate formed after about 20 minutes. TLC and MS flow injection confirmed completely conversion of starting materials. The mixture was cooled at room temperature and filtered and the solid was washed with ethanol (2 mL) to give 72 mg of compound **26** as a quite pure yellow solid that was converted directly in the

next step without further purification. Yield 60%. MS: m/z (ESI) calcd for $[C_{28}H_{20}BrFN_4O_2]^+$: 542.08, found 543 and 565 ($M+Na^+$).

3-bromo-N-(4-(((2-fluoro-4-(5-(2-oxo-2-(((4,4,5,5-tetramethyl-1,3,2-dioxaborolan-2-yl)methyl)amino)ethyl)-1H-benzo[d]imidazol-2-yl)phenyl)amino)methyl)phenyl)-4-methoxybenzamide (27a). Compound **27a** was prepared from **9a** by means of GP-H. **9a** (0.2 g, 0.33 mmol); R_f (EtOAc/MeOH 9:1): 0.8; 82% as a yellow solid; 200-201°C; washed with diethyl ether; IR *v* 3295 (NH), 1622 (C=O amide), 1600 (C=O amide) cm^{-1}. ^1H NMR (DMSO d_6) δ 1.06 (s, 12H, CH_3C), 2.13 (br d, 1H, CH_2B), 3.50 (s, 1H, Ar$\underline{CH_2}$CO), 3.70 (br d, 1H, CH_2B), 3.94 (s, 3H, OCH_3), 4.42-4.43 (d, 2H, Ar$\underline{CH_2}$NH J = 4 Hz), 6.72-6.81 (m, 2H, benzene H, and Ar-$NHCH_2$), 7.24 (t, 2H, benzimidazole C6-H and C4-H, J = 8 Hz), 7.36 (d, 2H, benzene H, J = 8 Hz), 7.59 (s, 1H, benzene H), 7.62 (d, 1H, benzimidazole C7-H, J = 8 Hz), 7.70-7.80 (m, 4H, benzene H), 8.00 (d, 1H, benzene H, J = 8 Hz), 8.22 (s, 1H, benzene H), 9.24 (br t, 1H, $CH_2\underline{NH}CO$), 10.17(s, 1H, NHCO), 12.94 (br s, 1H, imidazole H); MS: m/z (ESI) calcd for $[C_{37}H_{38}BBrFN_5O_5]^-$: 741.21, found: 766.65 (M^-+Na^+).

3-bromo-N-(4-(((2-fluoro-4-(5-(2-oxo-2-(((4,4,5,5-tetramethyl-1,3,2-dioxaborolan-2-yl)methyl)amino)ethyl)benzo[d]oxazol-2-yl)phenyl)amino)methyl)phenyl)-4-methoxybenzamide (27b). Compound **27b** was prepared from **10a** by means of GP-H. **10a** (0.2 g, 0.33 mmol); R_f (n-hexane/EtOAc 1:1): 0.5; 75% as an orange solid; 150-151°C; washed with diethyl ether; IR *v* 3298 (NH), 1651 (C=O amide), 1621 (C=O amide)cm^{-1}. ^1H NMR (DMSO d_6) δ 1.07 (s, 12H, CH_3C), 2.22 (br d, 1H, CH_2B), 3.52 (br d, 1H, CH_2B), 3.70 (s, 1H, Ar$\underline{CH_2}$CO), 3.94 (s, 3H, OCH_3), 4.44 (br d, 2H, Ph$\underline{CH_2}$NH), 6.76 (t, 1H, benzene H, J = 8 Hz), 7.11 (br t, 1H, $\underline{NH}CH_2$), 7.24 (t, 2H, benzoxazole C6-H and C4-H, J = 8 Hz), 7.36 (d, 2H, benzene H, J = 8 Hz), 7.59 (s, 1H, benzene H), 7.62 (d, 1H, benzoxazole C7-H,, J = 8 Hz), 7.70-7.80 (m, 4H, benzene

H), 8.00 (d, 1H, benzene H, J = 8 Hz), 8.22 (s, 1H, benzene H), 9.10 (br t, 1H, $CH_2\underline{NH}CO$), 10.18 (s, 1H, NHCO); MS: m/z (ESI) calcd for $[C_{37}H_{37}BBrFN_4O_6]^-$: 742.20, found: 742.67.

Methyl 2-(3-amino-4-hydroxyphenyl)acetate (28). Compound **28** was prepared according to literature.[22] Analytical data are herein reported.

4-Formylbenzoyl chloride (29). Compound **29** was prepared according to literature.[28] Analytical data are herein reported.

Methyl 2-(3-(4-formylbenzamido)-4-hydroxyphenyl)acetate (30). A solution of 4-formylbenzoyl chloride **29** (1.12 g, 6.67 mmol) in anhydrous CH_2Cl_2 (20 mL) was added drop wise to a well-stirred solution of **28** (1.2 g, 6.67 mmol) and Et_3N (1.34 g, 13.34 mmol, 1.86 mL) in anhydrous CH_2Cl_2 (100 mL) refrigerated in an ice-bath and the reaction was stirred at room temperature overnight. The mixture was diluted with CH_2Cl_2 and washed with water, $NaHCO_3$ s.s., 1N HCl and brine; the organic layer was dried on anhydrous Na_2SO_4, filtered and concentrated under reduced pressure to give a dark orange solid (1.7 g, 73%) directly used in the following step without further purification and characterization. R_f (*n*-hexane/ethyl acetate 3:7): 0.78.

Methyl 2-(2-(4-formylphenyl)benzo[d]oxazol-5-yl)acetate (31). To a well-stirred solution of **30** (2.44 g, 7.00 mmol) in toluene (20 mL) PTSA monohydrate (2.5 g, 14.7 mmol) was added and the mixture was stirred at 130° C for 3h. Water which formed was removed by the means of Dean-Stark apparatus. The organic phase was reduced under vacuum and the raw material was diluted with CH_2Cl_2 and washed with $NaHCO_3$ s.s. and brine; the organic layer was dried on anhydrous Na_2SO_4, filtered and concentrated under reduced pressure. The crude product was purified by column chromatography using chloroform/ethyl acetate 9:1 as eluent, to give the subtitle benzoxazole derivative as a yellow solid (0.76 g, 37%). R_f (chloroform/ethyl acetate 9:1):

0.59; 156 °C; cyclohexane; IR ν 1732 (C=O ester), 1701 (CHO) cm^{-1}; ^1H NMR ($CDCl_3$-*d*) δ 3.67 (s, 3H, CH_3), 3.72 (s, 2H, CH_2), 7.29 (d, 1H, J=8.8 Hz, C6-H benzoxazole), 7.51 (d, 1H, J=8.4 Hz, C7-H benzoxazole), 7.67 (s, 1H, C4-H benzoxazole), 7.98 (d, 2H, J=8.4 Hz, benzene H), 8.36 (d, 2H, J=8.4 Hz, benzene H), 10.05 (s, 1H, CHO). MS: m/z (ESI) calcd for $[C_{17}H_{13}NO_4]^+$: 295.08, found: 295.80.

Methyl 2-(2-(4-amino-3-fluorophenyl)benzo[d]oxazol-5-yl)acetate (32). Compound **32** was prepared according to literature.[22] Analytical data are herein reported.

Methyl (E)-2-(2-(3-fluoro-4-((4-(5-(2-methoxy-2-oxoethyl)benzo[d]oxazol-2-yl)benzylidene)amino)phenyl)benzo[d]oxazol-5-yl)acetate (33). Compound **33** was prepared from **31** by means of GP-F. **31** (1.35g 4.56 mmol); R_f (chloroform/ethyl acetate 1:1): 0.72; 87% as yellow solid; 276 °C; IR ν 1732 (C=O ester), 1631 (N=CH imine) cm^{-1}; ^1H NMR ($CDCl_3$-*d*) δ 3.65 (s, 6H, CH_3), 3.71 (s, 4H, CH_2), 7.25 (br d, 2H, C6-H benzoxazole), 7.47-7.52 (m, 3H, benzene H), 7.62-7.65 (m, 2H, C7-H benzoxazole and benzene H), 7.97-8.06 (m, 4H, C4-H benzoxazole, C7-H benzoxazole and benzene H), 8.31-8.34 (m, 2H, benzene H), 8.59 (s, 1H, N=CH); MS: m/z (ESI) calcd for $[C_{33}H_{24}FN_3O_6]^+$: 577.17, found: 578.

Methyl 2-(2-(3-fluoro-4-((4-(5-(2-methoxy-2-oxoethyl)benzo[d]oxazol-2-yl)benzyl)amino)phenyl)benzo[d]oxazol-5-yl)acetate (34). Compound **34** was prepared from **33** by means of GP-G. **33** (0.5 g, 0.86 mmol); 10 mL THF; R_f (chloroform/ethyl acetate 1:1): 0.68; 26% as a yellow solid; 265°C; washed with diethyl ether; IR ν 3374 (NH), 1729 (C=O ester) cm^{-1}; ^1H NMR ($CDCl_3$-*d*) δ 3.64 (s, 3H, CH_3), 3.65 (s, 3H, CH_3), 3.67 (s, 2H, CH_2), 3.69 (s, 2H, CH_2), 4.50 (br d, 2H, NHCH_2), 7.25 (t, 1H, J=8.4 Hz, benzene H), 7.15-7.23 (m, 2H, C6-H benzoxazole), 7.40 (d, 1H, J=8.4 Hz, C7-H benzoxazole), 7.45-7.48 (m, 3H, benzene H), 7.56 (s, 1H, C4-H benzoxazole), 7.61 (s, 1H, C4-H benzoxazole), 7.83-7.86 (m, 2H, C7-H

benzoxazole and benzene H), 8.18 (d, 2H, J=8 Hz, benzene H). MS: m/z (ESI) calcd for $[C_{33}H_{26}FN_3O_6]^+$: 579.18, found: 580.17.

Biological methods. *In vitro screening for Hpse activity*. To determine the activity of the Hpse inhibitors, a homogenous assay based on the cleavage of the synthetic heparin oligosaccharide Fondaparinux (Arixtra; Aspen) has been employed. The assay measures colorimetrically the appearance of the disaccharide product of Hpse-catalyzed fondaparinux cleavage, by using the tetrazolium salt WST-1. The assay was essentially performed as described[29] with minor modifications. Briefly, Nunc 96-well (Thermo Fisher Scientific) plates were pre-treated with a solution of 4% BSA (bovin serum albumin – Sigma-Aldrich) in phosphate-buffered saline containing 0.05% Tween 20 (PBST), for 2 h at 37°C and then washed three times with PBST.

The assay was carried out with 100 μL/well of assay solution containing 40 mM sodium acetate buffer (pH 5.0), 100 μM Fondaparinux, 2.5 nM recombinant Hpse (GS3) and serial dilutions of test compounds (tested in triplicate)(range of concentrations). Plates were sealed with adhesive tape and incubated, in the dark, for 3 h at 37°C, followed by development with 1.69 mM WST-1 (Santa Cruz biotechnology), for 1 h at 60°C. Then, the absorbance at 560 nm was measured through a microplate reader (Victor 3, Perkin Elmer).

IC_{50} value for each compound, versus Hpse, was calculated by GraphPad software. Finally, the measurements were corrected by subtracting both the reagent background and the inner absorbance value of test compound.

Cell lines and maintenance. HT1080 (fibrosarcoma), U87MG (glioblastoma) and U2OS (osteosarcoma) human cell lines were purchased from American Type Culture Collection (ATCC; Manassas ,VA) and maintained according to manufacturer's recommendations. Briefly, HT1080 and U87MG were grown in Modified Eagle Medium (Thermo Fisher Scientific), while

U2OS cells were grown in McCoy's 5a medium (Thermo Fisher Scientific), all supplemented with 10% FCS (Thermo Fisher Scientific), 100 U/mL penicillin and 100 µg/mL streptomycin (Thermo Fisher Scientific), 2 mM L-Glutamine (Thermo Fisher Scientific). All cell lines were maintained at 37°C with a humidified 5% CO_2 atmosphere.

The human synovial sarcoma cell line CME-1 was provided by M. Pierotti.[43] The human rhabdoid tumor cell line A204, obtained from ATCC, was authenticated by the AmpFISTR Identifiler PCR amplification kit (Applied Biosystems, PN4322288) and only pools of controlled cells were used. Both cell lines were cultured in RPMI medium (Lonza) supplemented with 10% FBS and maintained at 37 °C in 5% CO_2 atmosphere. Compound **15** was dissolved in 100% DMSO and diluted in cell culture (0.5% final concentration for CME- cells and 0.25% for A204 cells).

Proliferation assay. HT1080, U87MG and U2OS exponentially growing cells were seeded into 96-well plates and then, 24h later, treated with test compounds dissolved in DMSO or the solvent alone. Inhibition of cell proliferation was measured by means of a classical sulforhodamine B (SRB) assay performed in triplicate. The drug concentrations able to inhibit cell proliferation by 50% (IC_{50}) were ultimately calculated from dose–response curves, by using the GraphPad Prism 5.02 software.

Alternatively, exponentially growing CME-1 and A204 cells were seeded in 12 well/plates and, 24h later, treated with the drug dissolved in DMSO or the solvent alone. The antiproliferative activity was evaluated after 72h of drug exposure, by cell counting. IC_{50} values were calculated as above.

Matrigel invasion assay. Cells were pretreated with the indicated drug concentrations in complete medium for 24h. Then, cells were harvested, resuspended in serum-free medium and

transferred (2.5 x10^4 HT1080, U87MG and U2OS; 1.2 x10^5 CME-1 and 1.8 x10^5 A204 cells/filter, respectively) to the upper chamber of 24-well Transwell plates (Costar, Corning Inc., Corning, NY) previously coated with Growth Factor Reduced Matrigel (BD Biosciences, San Jose, CA). The same drug concentration used for cell pretreatment was added to both the upper and lower chambers. After 24h of incubation, cells that invaded the Matrigel were stained with SRB and then counted under a microscope, at 40X-100X magnification depending on cell density. Statistical analyses were performed by the Student's 2-tailed *t* test. $P<0.05$ was considered significant.

Real Time qPCR assay. Total RNA was extracted from HT1080 cells, upon 24 h treatment with test compounds (1 μM), and then retrotranscribed using the iScript™ Advanced cDNA Synthesis Kit for RT-qPCR (Bio-Rad Laboratories Inc., Hercules, CA) according to the manufacturer's instructions. Real Time quantitative PCR analysis was performed using SsoAdvanced Universal SYBR Green Supermix (Bio-Rad Laboratories Inc., Hercules, CA) and the following PrimePCR SYBR Green Assays: qHsaCID0015228 (HPSE-1), qHsaCED0002206 (FGF-1), qHsaCID0015510 (FGF-2), qHsaCID0011597 (MMP-9), qHsaCED0043454 (VEGF-A) (Bio-Rad Laboratories Inc., Hercules, CA). The 7900HT Sequence Detection System instrument and software (Applied Biosystems) were used to quantify the relative expression of the target genes by the ΔΔCt method using total RNA to normalize gene expression.

Computational protocol. Molecular modeling studies were performed with the Schrodinger 2015-4 software suite and with MODELLER 9.16.[34] Ligand molecules were built with Maestro 10.4[44] and prepared with LigPrep 3.6.[45] The protein structure was modelled with MODELLER 9.16 for the insertion of the GS3 peptide and refined with the Protein Preparation Wizard tool of

the Schrodinger suite. Docking studies were performed with Glide 6.9[46] using the SP scoring function.

Protein modeling and preparation. The structure of Hpse GS3 construct was modeled from the crystal coordinates of human Hpse in complex with the tetrasaccharide inhibitor dp4 (pdb code: 5E9C),[31] by inserting the octapeptide GSGSGSQK between the last amino acid (E109) of the 8 kDa chain and the first crystallized amino acid (K159) of the 50 kDa chain.[32] The loop was built using MODELLER 9.16 with default settings, leaving the terminal crystallized residues E109 and K159 flexible to allow proper geometries of construct. Different models were built and ranked according to their MOLPDF value. The best scoring models were very similar in terms of backbone arrangement and side chain orientations. The model with the lowest MOLPDF was used for docking studies. Before docking, the model was prepared using the Protein Preparation Wizard tool of Maestro Suite and energy minimized with its co-crystalized ligand (dp4) in the substrate binding site. In particular, the ligand was added to the model obtained from MODELLER and missing protein hydrogen atoms were added. The orientation of thiol and hydroxyl groups, the conformations of asparagine, glutamine and histidine residues were adjusted to optimize the overall hydrogen bonding network. Basic and acid amino acids were modeled in their charged form. H296, bridging two acidic groups, was modeled in its protonated form. The resulting structure was submitted to a first minimization run with the OPLS2005 force field[47] in which only hydrogen atoms were free to move. A second minimization was then performed on the whole structure, restraining the position of complex heavy atoms to an RMSD value of 0.3 Å.

Docking studies. The docking grid was built using Glide 3.9[34-36] and was centered on the position of the tetrasaccharide inhibitor dp4, setting the dimensions of bounding and enclosing

boxes to 15 and 50 Å, respectively. The binding poses were ranked according to the Emodel scoring function. The best ranked pose for each inhibitor was then merged into the protein structure and the complex was minimized with the OPLS2005 force field implemented in MacroModel 11.0, using the Polak-Ribiere conjugate gradient method to a convergence threshold of 0.05 kJ mol^{-1} $Å^{-1}$. During the minimization the ligands and residues within 8 Å from them were free to move, while the backbone of other residues was kept fixed.

Molecular Dynamics simulations. Molecular Dynamics simulations were performed using Desmond 4.8.[48] The protein was parametrized by applying the ff14SB Amber Force Field,[49] while the ligands were parametrized by applying the General Amber Force Field (GAFF).[50] Partial atomic charges of inhibitors were computed by the Antechamber module[51] of AmberTools 14 at the AM1-BCC level. The complexes were solvated with a box of TIP3P water, placing the box boundaries 12 Å far from the complex atoms on each side. The positive charge of the system was neutralized by adding Cl^- counterions. After a relaxation protocol implemented to progressively release the positional restraints applied to the heavy atoms of the complexes, 25 ns of unrestrained MD simulations were performed, using the Langevin[52] coupling scheme in the NPT ensemble, and setting the temperature at 300 K. Bond lengths to hydrogen atoms were constrained using M-SHAKE.[53] Short-range electrostatic interactions were cut off at 9 Å, whereas long-range electrostatic interactions were computed using the Smooth Particle Mesh Ewald method.[54] A RESPA integrator[55] was used with a time-step of 2 fs, and long-range electrostatics were computed every 6 fs. The molecular dynamics simulations were replicated two times by modifying the initial velocities of the atoms.

ASSOCIATED CONTENT

Supporting Information. The Supporting Information is available free of charge on the ACS Publications website at DOI:

Human Hpse GS3 construct, Hpse in complex with compounds **13a** and **13c**, values of docking scoring function for compounds **9a**, **10a**, **13a-c** and **14a-e**, RMSD values of derivatives **9a**, **10a**, **13a** and **14d**, details of HPLC analyses, HPLC traces of compounds **9a,b**, **10a,c**, **13a-d** and **14a-f**, pdb files of human GS3 Hpse model in complex with docking poses of compounds **9a**, **10a**, **13a** and **14d**.

Molecular formula strings and some data (CSV)

AUTHOR INFORMATION

Corresponding Author

*For R.D.S.: phone, +39-06-49913150; E-mail, roberto.disanto@uniroma1.it.

*For G.G.: phone, +39-06-91393640; E-mail, giuseppe.giannini@alfasigma.com.

ORCID

Valentina Noemi Madia: 0000-0002-5724-612X

Antonella Messore: 0000-0003-0158-5816

Luca Pescatori: 0000-0003-4734-7856

Francesco Saccoliti: 0000-0002-2907-5503

Valeria Tudino: 0000-0001-9024-9835

Martina Bortolami: 0000-0001-5740-6499

Luigi Scipione: 0000-0002-2006-7005

Roberta Costi: 0000-0002-1314-9029

Silvia Rivara: 0000-0001-8058-4250

Laura Scalvini: 0000-0003-3610-527X

Marco Mor: 0000-0003-0199-1849

Roberto Di Santo: 0000-0002-4279-7666

Giuseppe Giannini: 0000-0002-7127-985X

Author Contributions

The manuscript was written through contributions of all authors. All authors have given approval to the final version of the manuscript.

Notes

The authors declare no competing financial interest.

ACKNOWLEDGMENT

We thank Mrs Enrica Favini for technical support.

ABBREVIATIONS

HSPGs, heparan sulfate proteoglycans; ECM, extracellular matrix; HS, heparan sulfate; Hpse, heparanase; BM, basement membrane; CAN, ceric ammonium nitrate; EDCI, 1-ethyl-3-(3-

dimethylaminopropyl)carbodiimide hydrochloride; DMAP, 4-dimethylaminopyridine; DIPEA, *N*,*N*-diisopropylethylamine; TBTU, 2-(1*H*-Benzotriazole-1-yl)-1,1,3,3-tetramethylaminium tetrafluoroborate; PTSA, *p*-toluenesulfonic acid; Fmoc, fluorenylmethyloxycarbonyl; SAR, structure−activity relationship; ATIII, antithrombin III; HT1080, human fibrosarcoma cell line; U87MG, human glioblastoma astrocytoma cell line; U2OS, human osteosarcoma cell line; HBD-1, heparin binding domain 1; HBD-2, heparin binding domain 2; VEGF, vascular endothelial growth factor; MMP9, matrix metallopeptidase 9; FGF-1, fibroblast growth factor; GP, general procedure; IR, infrared.

REFERENCES

1. Rivara, S.; Milazzo, F. M.; Giannini, G. Heparanase: a rainbow pharmacological target associated to multiple pathologies including rare diseases. *Future Med. Chem.* **2016**, *8*, 647-680.

2. Li, J. P.; Kusche-Gullberg, M. Heparan sulfate: biosynthesis, structure, and function. *Int. Rev. Cell. Mol. Biol.* **2016**, *325*, 215-273.

3. Nakato, H.; Li, J. P. Functions of heparan sulfate proteoglycans in development: insights from drosophila models. *Int. Rev. Cell. Mol. Biol.* **2016**, *325*, 275-293.

4. Bishop, J. R.; Schuksz, M.; Esko, J. D. Heparan sulphate proteoglycans fine-tune mammalian physiology. *Nature* **2007**, *446*, 1030–1037.

5. Billings, P. C.; Pacifici, M. Interactions of signaling proteins, growth factors and other proteins with heparan sulfate: mechanisms and mysteries. *Connect. Tissue Res.* **2015**, *56*, 272-280.

6. Parish, C. R.; Freeman, C.; Hulett, M. D. Heparanase: a key enzyme involved in cell invasion. *Biochim. Biophys. Acta* **2001**, *1471*, M99-M108.

7. Khamaysi, I.; Singh, P.; Nasser, S.; Awad, H.; Chowers, Y.; Sabo, E.; Hammond, E.; Gralnek, I.; Minkov, I.; Noseda, I.; Neta I.; Vlodavsky, I.; Abassi, Z. The role of heparanase in the pathogenesis of acute pancreatitis: a potential therapeutic target. *Sci. Rep.* **2017**, *7*, 715.

8. Parish, C. R.; Freeman, C.; Ziolkowski, A. F.; He, Y. Q.; Sutcliffe, E. L.; Zafar, A.; Rao, S.; Simeonovic, C. J. Unexpected new roles for heparanase in type 1 diabetes and immune gene regulation. *Matrix Biol.* **2013**, *32*, 228-233.

9. Li, J. P.; Vlodavsky, I. Heparin, heparan sulfate and heparanase in inflammatory reactions. *Thromb. Haemostasis* **2009**, *102*, 823-828.

10. Ilan, N.; Elkin, M.; Vlodavsky, I. Regulation, function and clinical significance of heparanase in cancer metastasis and angiogenesis. *Int. J. Biochem. Cell Biol.* **2006**, *38*, 2018-2039.

11. Cassinelli, G.; Favini, E.; Dal Bo, L., Tortoreto, M.; De Magli, M.; Dagrada, G.; Pilotti, S.; Zunino, F.; Zaffaroni, N.; Lanzi, C. Antitumor efficacy of the heparan sulfate mimic roneparstat (SST0001) against sarcoma models involves multi-target inhibition of receptor tyrosine kinases. *Oncotarget.* **2016**, *7*, 47848-47863.

12. Vlodavsky, I.; Beckhove, P.; Lerner, I.; Pisano, C.; Meirovitz, A.; Ilan, N.; Elkin, M. Significance of heparanase in cancer and inflammation. *Cancer Microenviron.* **2012**, *5*, 115-132.

13. Pisano, C.; Vlodavsky, I.; Ilan, N.; Zunino, F. The potential of heparanase as a therapeutic target in cancer. *Biochem. Pharmacol*. **2014**, *89*, 12-19.

14. Shteingauz, A.; Boyango, I.; Naroditsky, I.; Hammond, E.; Gruber, M.; Doweck, I.; Ilan, N.; Vlodavsky, I. Heparanase enhances tumor growth and chemoresistance by promoting autophagy. *Cancer Res.* **2015**, *75*, 3946-3957.

15. Lanzi, C.; Zaffaroni, N.; Cassinelli, G. Targeting heparan sulfate proteoglycans and their modifying enzymes to enhance anticancer chemotherapy efficacy and overcome drug resistance. *Curr. Med. Chem.* **2017**, *24*, 2860-2886

16. Ramani, V. C.; Vlodavsky, I.; Ng M.; Zhang, Y.; Barbieri P.; Noseda, A.; Sanderson, R. D. Chemotherapy induces expression and release of heparanase leading to changes associated with an aggressive tumor phenotype. *Matrix Biol.* **2016**, *55*, 22-34.

17. Larrue, C.; Saland, E.; Boutzen, H.; Vergez, F.; David, M.; Joffre, C.; Hospital, M. A.; Tamburini, J.; Delabesse, E.; Manenti, S.; Sarry, J. E.; Récher, C. Proteasome inhibitors induce FLT3-ITD degradation through autophagy in AML cells. *Blood* **2016**, *127*, 882-892.

18. Levy, J. M.; Thorburn, A. Targeting autophagy during cancer therapy to improve clinical outcomes. *Pharmacol. Ther.* **2011**, *131*, 130-141.

19. Xu, Y. J.; Miao, H. Q.; Pan, W.; Navarro, E. C.; Tonra, J. .; Mitelman, S.; Camara, M. M.; Deevi, D. S.; Kiselyov, A. S.; Kussie, V.; Wonga, W. C.; Liua, H. *N*-(4-{[4-(1H-Benzoimidazol-2-yl)-arylamino]-methyl}-phenyl)-benzamide derivatives as small molecule heparanase inhibitors *Bioorg. Med. Chem. Lett.* **2006**, *16*, 404-408.

20. Liu, H.; Pan, W.; Xu, Y.-J. (Benzimidazol-2-yl)-phenyl-benzyl-amine Derivatives and Methods for Inhibiting Heparanase Activity. PCT Int. Pat. Appl. WO 2005/042496, 2005.

21. Courtney, S. M.; Hay, P. A.; Buck, R. T.; Colville, C. S.; Phillips, D. J.; Scopes, D. I.; Pollard, F. C.; Page, M. J.; Bennett, J. M.; Hircock, M. L.; McKenzie, E. A.; Bhaman, M.; Felix, R.; Stubberfieldm C. R.; Turner, P. R. Furanyl-1,3-thiazol-2-yl and benzoxazol-5-yl acetic acid derivatives: novel classes of heparanase inhibitor. *Bioorg. Med. Chem. Lett.* **2005**, *15*, 2295-2299.

22. Courtney, S. M.; Hay, P. A.; Scopes, D. I. Benzoxazole, Benzthiazole and Benzimidazole Acid Derivatives and their Use as Heparanase Inhibitors. PCT Int. Pat. Appl. WO 2004/046122, 2004.

23. Baloglu, E.; Bohnert, G. J.; Ghosh, S.; Lobera, M.; Schmidt, D., R.; Sung, L. Compounds and Methods. PCT Int. Pat. Appl. WO 2013/19682, 2013.

24. Bahrami, K.; Khodaei, M. M.; Naali, F. Mild and highly efficient method for the synthesis of 2-arylbenzimidazoles and 2-arylbenzothiazoles. *J. Org. Chem.* **2008**, *73*, 6835-6837.

25. Stigers, K. D.; Koutroulis, M. R.; Chung, D. M.; Nowick, J. Fmoc: a more soluble analogue of the 9-fluorenylmethoxycarbonyl protecting group. *J. Org. Chem.* **2000**, 65, 3858-3860.

26. Ivanov, A. S.; Zhalnina, A. A.; Shishkov, S. V. A convergent approach to synthesis of bortezomib: the use of TBTU suppresses racemization in the fragment condensation. *Tetrahedron* **2009**, *65*, 7105-7108.

27. Coutts, S. J.; Adams, J.; Krolikowski, D.; Snow, R. J. Two efficient methods for the cleavage of pinanediol boronate esters yielding the free boronic acids. *Tetrahedron Lett.* **1994**, *35*, 5109-5112.

28. Wong, D. Y. Q.; Lau, J. Y.; Ang, W. H. Harnessing chemoselective imine ligation for tethering bioactive molecules to platinum(IV) prodrugs. *Dalton Trans.* **2012**, *41*, 6104-6111.

29. Hammond, E.; Li, C. P.; Ferro, V. Development of a colorimetric assay for Hpse activity suitable for kinetic analysis and inhibitor screening. *Anal. Biochem.* **2010**, *396*, 112–116.

30. Schiemann, S.; Lühn, S.; Alban, S. Development of both colorimetric and fluorescence heparinase activity assays using fondaparinux as substrate. *Anal. Biochem.* **2012**, *427*, 82–89.

31. Levy-Adam, F.; Abboud-Jarrous, G.; Guerrini, M.; Beccati, D.; Vlodavsky, I.; Ilan, N. Identification and characterization of heparin/heparan sulfate binding domains of the endoglycosidase heparanase. *J. Biol. Chem*. **2005**, *280*, 20457-20466.

32. Wu, L.; Viola, C. M.; Brzozowski, A. M.; Davies G. J. Structural characterization of human heparanase reveals insights into substrate recognition. *Nat. Struct. Mol. Biol.* **2015**, *22*, 1016-1022.

33. Nardella, C.; Lahm, A.; Pallaoro, M.; Brunetti, M.; Vannini, A.; Steinkühler, C. Mechanism of activation of human heparanase investigated by protein engineering. *Biochemistry* **2004**, *43*, 1862–1873.

34. Fiser, A.; Do, R. K.; Sali, A. Modeling of loops in protein structures. *Protein Sci.* **2000**, *9,* 1753-1773.

35. Friesner, R. A.; Banks, J. L.; Murphy, R. B.; Halgren, T. A.; Klicic, J. J.; Mainz, D. T.; Repasky, M. P.; Knoll, E. H.; Shaw, D. E.; Shelley, M.; Perry, J. K.; Francis, P.; Shenkin, P. S. Glide: A new approach for rapid, accurate docking and scoring. 1. Method and assessment of docking accuracy. *J. Med. Chem.* **2004**, *47*, 1739–1749.

36. Halgren, T. A.; Murphy, R. B.; Friesner, R. A.; Beard, H. S.; Frye, L. L.; Pollard, W. T.; Banks, J. L., Glide: a new approach for rapid, accurate docking and scoring. 2. Enrichment factors in database screening. *J. Med. Chem.* **2004**, *47*, 1750–1759.

37. Ishida, K.; Hirai, G.; Murakami, K.; Teruya, T.; Simizu, S.; Sodeoka, M.; Osada, H. Structure-based design of a selective heparanase inhibitor as an antimetastatic agent. *Mol. Cancer Ther.* **2004**, *3*, 1069-1077.

38. Zetser, A.; Bashenko, Y.; Miao, H. Q.; Vlodavsky, I.; Ilan, N. Heparanase affects adhesive and tumorigenic potential of human glioma cells. *Cancer Res.* **2003**, *63*, 7733-7741.

39. Cassinelli, G.; Lanzi, C.; Tortoreto, M.; Cominetti, D.; Petrangolini, G.; Favini, E.; Zaffaroni, N., Pisano, C.; Penco, S.; Vlodavsky, I.; Zunino, F. Antitumor efficacy of the heparanase inhibitor SST0001 alone and in combination with antiangiogenic agents in the treatment of human pediatric sarcoma models. *Biochem. Pharmacol.* **2013**, *85*, 1424-1432.

40. Cassinelli, G.; Dal Bo, L.; Favini, E.; Cominetti, D.; Pozzi, S.; Tortoreto, M.; De Cesare, M.; Lecis, D.; Scanziani, E.; Minoli, L.; Naggi, A.; Vlodavsky, I.; Zaffaroni, N.; Lanzi, C. Supersulfated low-molecular weight heparin synergizes with IGF1R/IR inhibitor to suppress synovial sarcoma growth and metastases. *Cancer Lett.* **2018**, *415*, 187-197.

41. Chen, L.; Sanderson, R. D. Heparanase regulates levels of syndecan-1 in the nucleus. *PLoS One* **2009**, *4*, e4947.

42. Schubert, S. Y.; Ilan, N.; Shushy, M.; Ben-Izhak, O.; Vlodavsky, I.; Goldshmidt, O. Human heparanase nuclear localization and enzymatic activity. *Lab. Invest*. **2004**, *84*, 535-544.

43. Tamborini, E.; Agus, V.; Mezzelani, A.; Riva, C.; Sozzi, G.; Azzarelli, A.; Pierotti, M. A.; Pilotti, S. Identification of a novel spliced variant of the SYT gene expressed in normal tissues and in synovial sarcoma. *Br. J. Cancer* **2001**, *84*, 1087-1094.

44. Schrödinger Release 2015-4. *Maestro*; Schrödinger, LLC: New York, 2015.

45. Schrödinger Release 2015-4. *LigPrep*; Schrödinger, LLC: New York, 2015.

46. Schrödinger Release 2015-4. *Glide*; Schrödinger, LLC: New York, 2015.

47. Kaminski, G. A.; Friesner, R. A.; Tirado-Rives, J.; W. Jorgensen, W. L. Evaluation and reparametrization of the opls-aa force field for proteins via comparison with accurate quantum chemical calculations on peptides. *J. Phys. Chem. B* **2001**, *105*, 6474–6487.

48. Schrödinger Release 2016-4. *Desmond Molecular Dynamics System*; D. E. Shaw Research: New York, 2016. *Maestro-Desmond Interoperability Tools*; Schrödinger: New York, 2016.

49. Case, D. A.; Babin, V.; Berryman, J. T.; Betz, R. M.; Cai, Q.; Cerutti, D. S.; Cheatham, III, T. E.; Darden, T. A.; Duke, R. E.; Gohlke, H.; Goetz, A. W.; Gusarov, S.; Homeyer, N.; Janowski, P.; Kaus, J.; Kolossváry, I.; Kovalenko, A.; Lee, T. S.; LeGrand, S.; Luchko, T.; Luo, R.; Madej, B.; Merz, K. M.; Paesani, F.; Roe, D. R.; Roitberg, A.; Sagui, C.; Salomon-Ferrer, R.; Seabra, G.; Simmerling, C. L.; Smith, W.; Swails, J.; Walker, R. C.; Wang, J.; Wolf, R. M.; Wu X; Kollman P. A. *AMBER 14*, University of California, San Francisco, 2014.

50. Wang J.; Wolf R. M.; Caldwell J. W.; Kollman P. A.; Case D. A. Development and testing of a general amber force field. *J. Comput. Chem.* **2004**, *25*, 1157-1174.

51. Wang J.; Wang, W.; Kollman P. A.; Case D. A. Automatic atom type and bond type perception in molecular mechanical calculations. *J. Mol. Graph. Model.* **2006**, *25*, 247–260.

52. Feller, S. E.; Zhang, Y.; Pastor, R. W.; Brooks, B. R. Constant pressure molecular dynamics simulation: the Langevin piston method. *J. Chem. Phys.* **1995**, *103*, 4613–4621.

53. Lippert, R. A.; Bowers, K. J.; Dror, R. O.; Eastwood, M. P.; Gregersen, B. A.; Klepeis, J. L.; Kolossvary, I.; Shaw, D. E. A common, avoidable source of error in molecular dynamics integrators. *J. Chem. Phys.* **2007**, *126*, 046101.

54. Essmann, U.; Perera, L.; Berkowitz, M. L.; Darden, T.; Lee, H.; Pedersen, L. G. A smooth particle mesh Ewald method. *J. Chem. Phys*. **1995**, *103*, 8577–8593.

55. Tuckerman, M.; Berne, B. J.; Martyna, J. Reversible multiple time scale molecular dynamics *J. Chem. Phys*. **1992**, *97*, 1990–2001.

For Table of Contents Only